

UNIVERSITY OF MINES AND TECHNOLOGY
TARKWA

FACULTY OF GEOSCIENCES AND ENVIRONMENTAL STUDIES
DEPARTMENT OF GEOMATIC ENGINEERING

A THESIS REPORT ENTITLED

ARTIFICIAL INTELLIGENCE APPROACH TO COORDINATE
TRANSFORMATION USING GROUP METHOD OF DATA HANDLING
AND LEAST SQUARE SUPPORT VECTOR MACHINE

BY
ROLAND TROKON GBATEA, JR

SUBMITTED IN PARTIAL FULFILLMENT OF THE REQUIREMENTS
FOR THE AWARD OF THE DEGREE OF MASTER OF SCIENCE IN
GEOMATIC ENGINEERING

THESIS SUPERVISORS

.....
ASSOC PROF SAVIOUR MARTEY

.....
DR Y.Y. ZIGGAH

TARKWA, GHANA
NOVEMBER 2023

DECLARATION

I declare that this thesis is my work. It is being submitted for the degree of Master of Science in Geomatic Engineering at the University of Mines and Technology, Tarkwa. It has not been submitted for any degree or examination in any other University.

.....

(Signature of Candidate)

..... Day of, 2023



ABSTRACT

Transforming coordinates from the WGS84 datum to the Accra 1929 reference frame is still a problem for geospatial professionals in Ghana, as long as Ghana has not moved to the geocentric datum. This research applied the Bursa-Wolf transformation model to determine transformation parameters, changed the World Geodetic System 1984 (WGS84) points to the Accra datum and then projected the transformed coordinates onto the Transverse Mercator 1° NW projection system being used in Ghana. The Bursa-Wolf results were compared to the Group Method of Data Handling (GMDH) and the Least Square Support Vector Machine (LS-SVM). For all methods, the geodetic coordinates of the global system were transformed to the geodetic coordinates of the War Office before projection. To get the optimal performance of the model, the K-fold cross-validation approach was applied. Thirty-four points were used and divided into five folds. The average of the horizontal positional error of the five-folds gave the model the best output. The result reveals that the LS-SVM, GMDH and the Bursa-Wolf models average root mean square horizontal positional error of 2.5541, 3.0312, 3.3396, respectively; average mean horizontal positional error of 2.1904, 2.6191, 2.7578; and averaged standard deviation of 1.7, 2.139, 2.3563 respectively. It shows that LS-SVM is of best performance than the GMDH and the Bursa-Wolf model. Since the horizontal error of the LS-SVM is higher than the allowable ± 0.9114 m standard for horizontal measurement in Ghana, the LS-SVM was recommended to be used for only low-order surveys like data collection for GIS databases, and topographic surveys.

ACKNOWLEDGEMENTS

I am grateful to the Almighty God for the privileges of Life that I enjoy and the ability He has given me.

So many thanks go to ArcelorMittal Mining Company (Liberia) for their full sponsorship throughout my study. You will remain in my heart forever for your support to me in pursuing a Master's degree in Geomatic Engineering.

To brilliantly come out with this topic and complete it, it was the help of Dr Y.Y. Ziggah and Assoc. Prof. Saviour Mantey. I salute you all! Without you, I could have not completed this work; many thanks. May God richly bless you and your entire families.

Thanks to all my lecturers, the teaching assistants, and friends who directly or indirectly contributed to this research.

Appreciate every one of you!

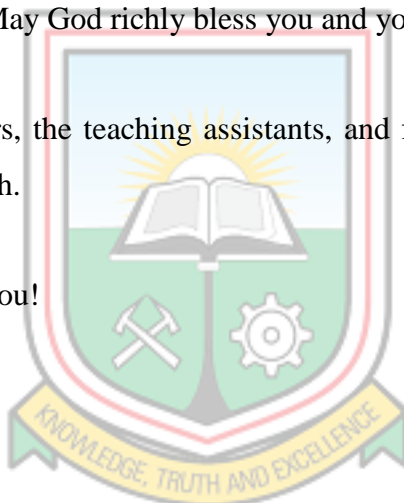


TABLE OF CONTENTS

Contents	Page
DECLARATION	i
ABSTRACT	ii
ACKNOWLEDGEMENTS	iii
TABLE OF CONTENTS	iv
LIST OF FIGURES	vii
LIST OF TABLES	viii
CHAPTER 1 INTRODUCTION	1
1.1 Problem Statement	1
1.2 Objectives of Thesis	2
1.3 Methods Used	2
1.4 Resources Used	3
1.5 Organisation of Thesis	3
CHAPTER 2 RELEVANT INFORMATION ABOUT THE STUDY AREA	4
2.1 Location	4
2.2 Topography	4
2.3 Climate	5
2.4 Ghana's Geodetic Reference Frame	5
CHAPTER 3 LITERATURE REVIEW	7
3.1 Earth Reference Surfaces	7
3.1.1 The Spherical (globe) Model	7
3.1.2 The Ellipsoidal Model	8
3.1.3 The Real Earth (Geoid) Model	8
3.2 Geodetic Datum	10
3.2.1 Horizontal Datum	10
3.2.2 Vertical Datum	11
3.2.3 Geocentric (Global) Datum	11
3.2.4 Non-Geocentric (Local) Datum	12

3.3	Coordinate System	12
3.3.1	Geodetic (Ellipsoidal) Coordinate System	13
3.3.2	Geocentric (Cartesian) Coordinate System	13
3.3.3	Modern GPS Coordinate System	14
3.4	Coordinate Conversion	15
3.4.1	Forward Conversion	15
3.4.2	Reverse Conversion	15
3.5	Coordinate Transformation	16
3.5.1	Three-Dimensional Transformation	17
3.5.2	Artificial Intelligence	18
3.6	Map Projection	21
3.6.1	Mercator Projection	22
3.6.2	Transverse Mercator Projection	23
3.6.3	Universal Transverse Mercator Projection (UTM)	24
3.6.4	Geography Coordinates to Projected Coordinates	24
3.7	Review of Application of Artificial Intelligence in Coordinate Transformation	26
CHAPTER 4 RESOURCES AND METHODS USED		30
4.1	Resources Used	30
4.1.1	Data DescriptionBV	30
4.2	Method Used	31
4.2.1	Forward Conversion	32
4.2.2	Bursa – Wolf Transformation	33
4.2.3	Reverse Conversion	34
4.2.4	Group Method of Data Handling	35
4.2.5	Least Square Support Vector Machine	35
4.2.6	The K-Fold Cross Validation	36
4.3	Model Performance	36
4.3.1	Root Mean Square Error	37
4.3.2	Root Mean Square of the horizontal Position Error	37
4.3.3	Horizontal Position Error	37
4.3.4	Standard Deviation	38

CHAPTER 5	RESULTS AND DISCUSSION	39
5.1	Results	39
5.1.1	Numerical Transformation Model Results	39
5.1.2	AI and Numerical Transformation Performance Results	46
5.2	Discussion	48
5.2.1	Bursa-Wolf Model	48
5.2.2	GMDH and LS-SVM Models	48
5.2.3	Comparison Between AI Models and Bursa-Wolf Models	49
CHAPTER 6	CONCLUSIONS AND RECOMMENDATIONS	50
6.1	Conclusions	50
6.2	Recommendations	50
REFERENCES		52
APPENDICES		57
APPENDIX A	COMMON POINTS WITH COORDINATES	58
APPENDIX B	BURSA-WOLF CODE	59
APPENDIX C	GROUP METHOD DATA HANDLING CODE	62
APPENDIX D	LEAST SQUARE SUPPORT VECTOR MACHINE CODE	63
APPENDIX E	PROJECTION CODE	64
INDEX		66

LIST OF FIGURES

Figure	Title	Page
Figure 2.1	Map of Ghana	4
Figure 3.1	Earth Spherical Model	7
Figure 3.2	Geoid Model of the Earth	9
Figure 3.3	Ellipsoidal, Geoid and the Earth Surface Relationship	9
Figure 3.4	Geocentric Datum	11
Figure 3.5	A Local Datum	12
Figure 3.6	Geodetic Coordinate System	13
Figure 3.7	Geocentric Coordinate System	14
Figure 3.8	The WGS 84 Coordinate System	15
Figure 3.9	Geometry of Bursa-Wolf Transformation	17
Figure 3.10	A Schematic Diagram of a Biological Neuron	19
Figure 3.11	Basic GMDH Structure	20
Figure 3.12	Projection Surfaces of Map Projection	22
Figure 3.13	Cylinder Orientation for the Transverse Mercator Projection	23
Figure 4.1	Map of Ghana Showing the Research Points	31
Figure 4.2	The Study's Flow Chart	32
Figure 5.1.	Diagram of the Training Residuals of Bursa-Wolf Model	39
Figure 5.2	Horizontal Position Residuals for Fold 1 (Training)	41
Figure 5.3	Horizontal Position Residuals for Fold 2 (Training)	42
Figure 5.4	Horizontal Position Residuals for Fold 3 (Training)	42
Figure 5.6	Horizontal Position Residuals for Fold 5 (Training)	43
Figure 5.5	Horizontal Position Residuals for Fold 4 (Training)	43
Figure 5.7	Horizontal Position Residuals for Fold 1 (Testing)	44
Figure 5.8	Horizontal Position Residuals for Fold 2 (Testing)	44
Figure 5.9	Horizontal Position Residuals for Fold 3 (Testing)	45
Figure 5.10	Horizontal Position Residuals for Fold 4 (Testing)	45
Figure 5.11	Horizontal Position Residuals for Fold 5 (Testing)	46
Figure 5.12	Statistical Indicators (Average) of all Folds and Model (Training)	47
Figure 5.13	Average Plot of All Folds and Models (Testing)	47

LIST OF TABLES

Table	Title	Page
Table 3.1	Parameter of Some Ellipsoid In Use	8
Table 4.1	Descriptive Statistic of Common Points	30
Table 4.2	Five Folds Cross Validation Technique Structure	36
Table 5.1	Transformation Parameter from Bursa-Wolf Model	39
Table 5.2	The Horizontal Residual's Performance Metric for Fold 1-4	40
Table 5.3	The Horizontal Residual's Performance Metric or Fold 4 and Fold 5	41
Table 5.4	Performance Metric for All Folds and Models (Average)	46



CHAPTER 1

INTRODUCTION

1.1 Problem Statement

It is noteworthy that the Global Navigation Satellite System (GNSS) technology, specifically the American Satellite system that is widely used, is configured to the World Geodetic System 1984 (WGS 84) datum; while Ghana adopts two local datums known as the Accra 1929 Datum and the Legon 1977 Datum (Kumi-Boateng and Ziggah, 2020a). The ellipsoid realised by the Accra datum is the War Office 1926, and the ellipsoid realised by the Legon 1977 Datum is the Clark 1880 (modified) (Kumi-Boateng and Ziggah, 2020a). The WGS84, which is a global datum, and the Accra 1929 datum are completely distant due to the difference in datum size, shape, and origin (Ayer, 2008). As Ghana utilises the GNSS technology for most of its survey works, it is imperative to change from the WGS84 reference frame to Accra 1929 reference frame for data compatibility. In doing that, data associated with the global datum will be commensurate with the local geodetic datum. The transfer of coordinates between the universal and local datums is an age-old challenge in geoscience, with Ghana being affected. The geodetic framework of Ghana has been identified as extremely warped due to a variety of problems with the local geodetic networks' setting up and the quality of the data they produce in general (Ayer, 2008; Ayer and Fosu, 2008; Poku-Gyamfi, 2009).

Existing studies (Solomon, 2013; Laari *et al.*, 2016; Ziggah and Yakubu, 2017;) have presented a series of numerical methods like the geocentric translation model, Abridged Molodesnky, Molodensky-Badekas, Bursa-Wolf, the Veis, and models for transforming coordinates. These mathematical models have helped geodesists and geospatial professionals to perform coordinate transformations between different reference datums. However, these aforementioned transformation models are limited because of their inadequacy in handling the distortion associated with spatial data having link with two unlike datums (Tierra *et al.*, 2008). Moreover, the models cannot be implemented without the determination of transformation parameters. Hence, there is always the need to have a functional relationship between the datums before it can be applied.

Literature has revealed that geospatial scientists are adopting Artificial Intelligence (AI) as a modern alternative approach to numerical models for coordinate transformation (Kumi-Boateng and Ziggah, 2020b). This is due to its robustness, nonparametric form, and ability to handle the distortion associated with spatial data between different datums (Ziggah *et al.*, 2017). Moreover, AI methods allow users to significantly train the data to predict an output with a desired error without any parametric relationship established. Unlike the traditional transformation models, the AI do not need transformation parameters to perform coordinate transformation. Because of the strength of AI, its application could benefit the geospatial sector of Ghana with accurate positioning information that aids in good estimation of volumes and areas, accurate boundaries demarcation, and promotes proper planning, management, and decision-making about the land and natural resources. In the light of that, the study applied two AI methods to transform coordinates from the WGS84 to the Accra 1929 datum. The methods employed include Group Method of Data Handling (GMDH) and Least Square Support Vector Machine (LS-SVM).

1.2 Objectives of the Thesis

The objectives of this study are to:

- i. Determine transformation parameters for the study area using a numerical approach;
- ii. Develop AI models to perform coordinate transformation;
- iii. Compare the results of the classical and AI models; and
- iv. Determine the best transformation model using statistical performance indicators.

1.3 Methods Used

The following methods were used to efficiently complete this research:

- Literature review;
- Numerical transformation model to determine the parameters and to perform the transformation;
- Artificial intelligence approach to transform coordinate precisely, GMDH and LS-SVM;
- Compare the best results from the numerical model (Bursa-wolf) to the Artificial Intelligence models using some statistical indicators; and

- Analysis of the results.

1.4 Resources Used

The following were the resources used for this research:

- Secondary data of common points of geodetic coordinates from Ghana Survey and Mapping Division of Lands Commission;
- MATLAB 2022b from the Computer Science Department;
- Internet facilities at UMaT.

1.5 Organisation of Thesis

This thesis is arranged into six chapters (1 – 6). Chapter One identifies the problem of coordination transformation in Ghana, the objectives of the study, research methods used for the study, and resources used. Chapter Two gives the overview of the study area in terms of its location, topography and climate. Relevant literatures on the topic are given in Chapter Three, where Ghana's Geodetic Reference frame is reviewed, earth surfaces, Geodetic Datums, Coordinates Systems, Coordinates Operation and Map Projection are discussed. Chapter Four reveals the resources and details of the method used for this thesis. Chapter Five presents results obtained from the study, which include: determined parameters, tables, graphs of all models, and Performance metric as well as the discussion associated with them. Chapter Six summarises the entire research with conclusion and recommendation as the main component.

CHAPTER 2

RELEVANT INFORMATION ABOUT THE STUDY AREA

2.1 Location

Ghana is a nation in West Africa that spans up to 536 km from east to west between longitudes 3° W and 1° E and 672 km from north to south between latitudes 4.5° N and 11° N. Cote d'Ivoire, on the west; Burkina Faso, to the north; and Togo, to the south are its neighbors (Mugnier, 2000). The regional map of Ghana in Figure 2.1 shows covered and uncovered regions of the study.

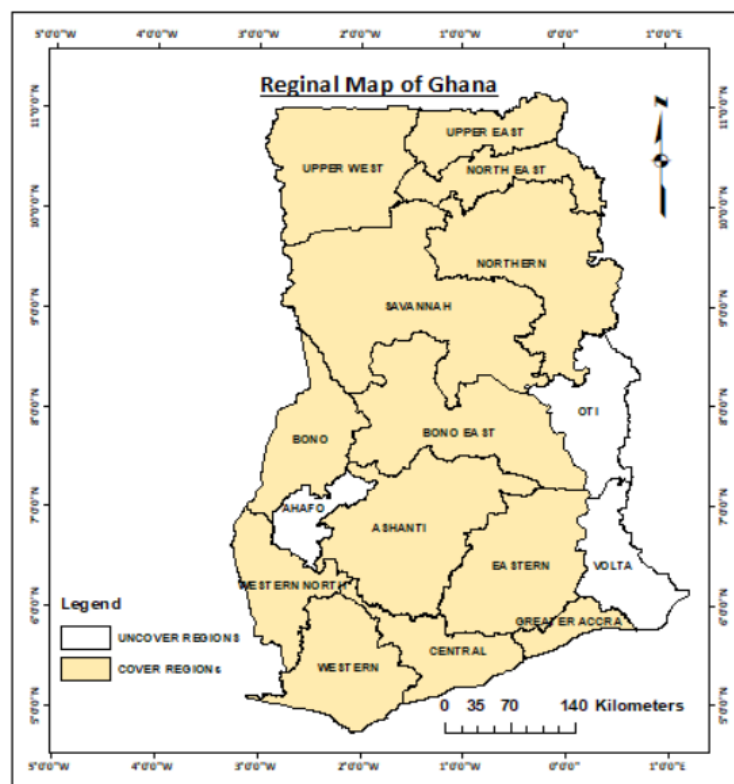


Figure 2.1 Map of Ghana (Author's Construct)

2.2 Topography

The landscape of Ghana consists of desert mountains, and the Kwahu plateau is located in the south-central region. The highest point in the Kwahu plateau is 883 m above sea level, whereas half of Ghana is below 152 m. The majority of the 537 km of coastline of sandy shore, support by grasslands and bush, and cut by a number of rivers and streams, that can be accessed by canoe. A tropical rain forest that continues northward from the shore, close

to the Ivory Coast border, and is divided by highly forested hills and numerous streams and rivers. The majority of Ghana's minerals, lumber, and cocoa are produced in this region, known as the "Ashanti." Low bushes, park-like savanna, and grassy plains cover the height, between from 91 m to 396 m above sea level, north of this region.

2.3 Climate

The tropical climate of Ghana ranges in temperature from 21° C to 32° C. Rainy months include April through July and September through November. On the shore, annual rainfall surpasses 200 cm, with a decline inland. For coastal west Africa, Accra's annual rainfall average of 76 cm is low. Most of the year, the country's southern region is humid, whereas the northern region is quite dry.

2.4 Ghana's Geodetic Reference Frame

In Ghana, the geodetic datums for cadastral activities are the Legon 1977 datum and Accra 1929 datum (Poku-Gyamfi, 2009; Ziggah *et al.*, 2019)]. The War Office 1926 ellipsoid serves as the basis for the Accra 1929 datum, while the Clarke 1880 (modified) ellipsoid serves as the basis for the Legon 1977 datum (Kumi-Boateng and Ziggah, 2020a). Sir Frederick Gordon Guggisberg, the Gold Coast Colony's previous governor started the nation's geodetic survey in June 1904. With a final estimated azimuth error of 0.360", the Governor's use of a zenith telescope to measure latitude from a pillar within the grounds of the Secretary of Native Affairs' home in Accra (Poku-Gyamfi, 2009) produced accurate results. The Gold Coast Survey (G.C.S.) 547's longitude was determined by the transmission of telegraphic signals with Cape Town, South Africa, in November and December of that same year (Mugnier, 2000). Despite the fact that the effect of local attractions was noticed in subsequent monitoring, the G.C.S. 547 (Accra), with latitude 5° 23' 43.33" N and longitude 0° 11' 52.3" W, was chosen as the beginning point for latitude and longitude for the then Gold Coast Colony. It was eventually discovered that a more practical system than geographic coordinates was required for the purpose of surveying and mapping. This led to adopting a Ghana Grid, a Transverse Mercator (TM) projection [(Mugnier, 2000) and (Poku-Gyamfi, 2009)]. Ghana's adopted Transverse Mercator projection has a longitude of 1° 00' 00" as its central meridian and a latitude of 4° 40' N. Avoiding negative coordinates from being generated, a False Easting of 274319.736 m was

added to any Y coordinates with a False Northing of zero. It was observed that a scale factor of 0.99975 was better appropriate at the longitude of origin (Kumi-Boateng and Ziggah, 2020b).



CHAPTER 3

LITERATURE REVIEW

3.1 Earth Reference Surfaces

Earth models are approximate sizes and shapes of the earth. An earth model is necessary to convert measurements obtained on the curved earth into maps or databases. Each model has benefits and drawbacks. Each is usually to some extent erroneous. Some of these errors are due to the design of the model rather than the measurements used to generate it. The three commonly used models of the earth (Clynch, 2002) are:

- The Spherical (globe) model
- The ellipsoidal model
- The Real Earth (Geoid) model

3.1.1 The Spherical (globe) Model

The globe is a fine representation of the earth in an elementary discussion of the earth. The sphere is the figure that lower the potential energy of the gravitational attraction of all the little mass elements for each other (Clynch, 2002). The spherical model shows how oblate the earth is; flatten at the poles and widen at the side. Figure 3.1 shows the earth spherical Model.



Figure 3.1 Earth Spherical Model (Bezdek and Sebera, 2013)

3.1.2 The Ellipsoidal Model

The ellipsoid is a model of the earth because the earth rotates. The Earth's rotating and gravitational forces combine to cause it to be slightly flattened near the poles, and the Earth's gravity fields gently undulating equipotential surfaces share this trait. A better reference surface is an ellipsoid, which is defined in geodesy as a surface of revolution formed by rotating an ellipse about its minor axis. Ziggah (2017) claimed that ellipsoids with specific geometric qualities can be situated in specific ways to be approximations of the global geoid or approximations of regional portions of the geoid, giving rise to geocentric or local reference ellipsoids.

Jessen (2009) stated that, “the geoid is computationally very complex, it is necessary to approximate it by a surface that can efficiently be handled mathematically, i.e. an ellipsoid of revolution (sometimes also called spheroid)”. Ellipsoids are characterized by two essential parameters, the size parameter, the semi-major axis, a and the shape parameter, eccentricity e or flattening f . A table of some common ellipsoids are given in Table 3.1.

Table 3.1 Parameter of Some Ellipsoid In Use (Source: Jessen, 2009)

Ellipsoid	Semi-major axis a (m)	Inverse flattening
Airy 1830	6,377,563.396	299.3249646
ANS	6,378,160.000	298.25
Bessel 1841	6,377,397.155	299.1528128
Clarke 1866	6,378,206.400	294.9786982
Clarke 1880	6,378,249.145	293.465
GRS80	6,378,137.00	298.257222101
International 1924	6,378,388.00	297.0
WGS84	6,378,137.00	298.257223563
War Office 1926	6,378,299.99899832	296

3.1.3 The Real Earth (Geoid) Model

The geoid, a specific equipotential surface, represents the worldwide mean sea level, and because seas and oceans comprise roughly 70% of the Earth's surface, the geoid is a close approximation of the Earth's true shape (Ziggah, 2017). The real earth model is a smoothly undulating surface that is challenging to define mathematically, making it ineffective as a

computational surface of reference. It is used for geodetic, geophysical, oceanographic and precise engineering applications (Mirghasempour and Joodaki, 2008). Figure 3.2 illustrates the geoid model.

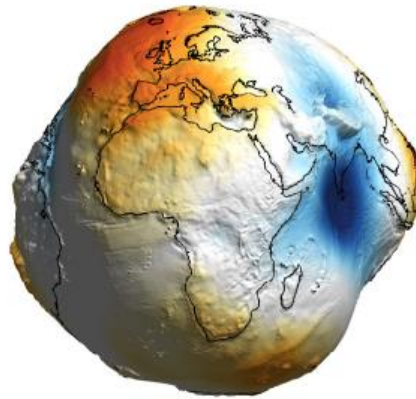


Figure 3.2 Geoid Model of the Earth (Bezdek and Sebera, 2013)

An important component in the position determination of any point is its height. The Global Positioning System (GPS) accurately derives the horizontal and vertical position of points on the earth's surface. The height captured by the GPS is the ellipsoidal height, which has its reference as the WGS84 ellipsoid, and is a global surface that represents the earth for geodetic computation since the geoid has an undulating nature. The geoid is used to estimate the physical shape of the Earth; it is the equipotential platform of the Earth's gravity field (Borge, 2013). Using the geoid as a reference surface, the height obtained is the orthometric height. Vermeer (2019) term it as the height above sea surface. The geoidal and ellipsoidal heights are mathematically defined in Equation (3.1) as:

$$H = h - N \quad (3.1)$$

where, H is the orthometric height, h is the ellipsoid height, and N is the geoidal height/geoidal undulation. The pictorial view of difference between the ellipsoid, earth surface and geoid are given in Figure 3.3.

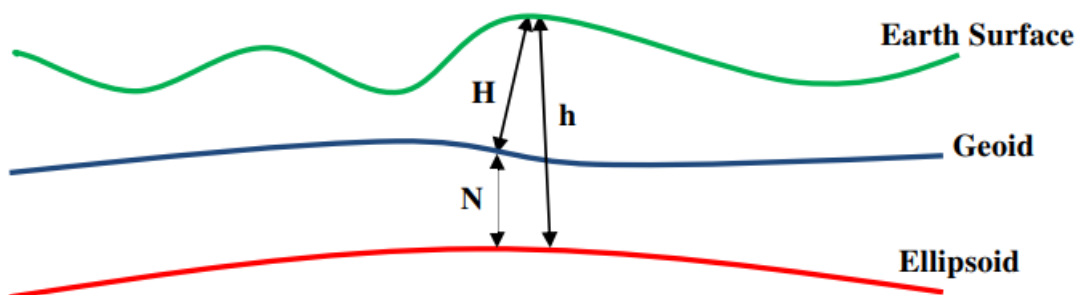


Figure 3.3 Ellipsoidal, Geoid and the Earth Surface Relationship (Eteje *et al.*, 2018)

3.2 Geodetic Datum

A datum is a reference surface and framework of the Earth's surface against which positional measurements are obtained for computing locations in geoscience (Dhungana and Lama, 2014). A geodetic datum is primarily composed of horizontal and vertical datums, gravity datums as well as sounding datums. Geodetic datums serve as the framework and provide starting information for geospatial activities.

To establish and maintain the elevation framework (vertical control network), coordinate framework (horizontal and satellite geodetic control networks), and gravimetric framework (gravity control network) geodetic datums are needed. Reasons for establishing a datum include defining a coordinate system, height system, and gravity reference system (Ziggah, 2017). Traditional geodetic techniques use various datum to determine the horizontal coordinates and heights of locations on the Earth's surface. Datum can be classified as:

- Horizontal Datum
- Vertical Datum
- Geocentric Datum
- Non-Geocentric Datum



3.2.1 Horizontal Datum

Horizontal datums consist of a network of control monuments whose horizontal positions have been determined by precise geodetic control surveys (Ghilani and Wolf, 2012). The establishment of a geodetic control network separates the horizontal from the vertical control network. The horizontal control network establishes the horizontal datum of a surface location. The datum itself is made up of a large number of survey markers that have been precisely surveyed and adjusted together to provide a consistent network of horizontal control from which all other horizontal measures can be derived. (Ghilani and Wolf, 2012).

3.2.2 Vertical Datum

Vertical datum serves as a foundation for elevation measurements and is used in a variety of spatial applications such as floodplain management, waterway navigation management, roadway and drainage design, agricultural management, and surveying in general (Jessen, 2009). A vertical datum can also be defined as a base measurement point (or set of points) from which all elevations are referred.

Vertical datum is important because all elevations need to be referenced to the same system. Without a vertical control framework, surveyors would calculate different elevation values for the same location. There are three kinds of vertical datums (geoid, quasi-geoid, reference ellipsoid) which are used in geodesy: the geoid, reference for orthometric and dynamic heights; the quasi geoid, reference surface for normal height; and the reference ellipsoid, reference surface for geodetic (geometric) height. A vertical datum is a zero-height surface of the national height system generally defined by mean sea level.

3.2.3 Geocentric (Global) Datum

The datum that most closely resembles the form and size of our planet is called the geocentric datum. Its ellipsoid's centre lines up with the mass axis of the Earth. In general, the geocentric datum is a decent fit for the earth as a whole, but not for a specific area. Figure 3.4 illustrates a Geocentric datum.

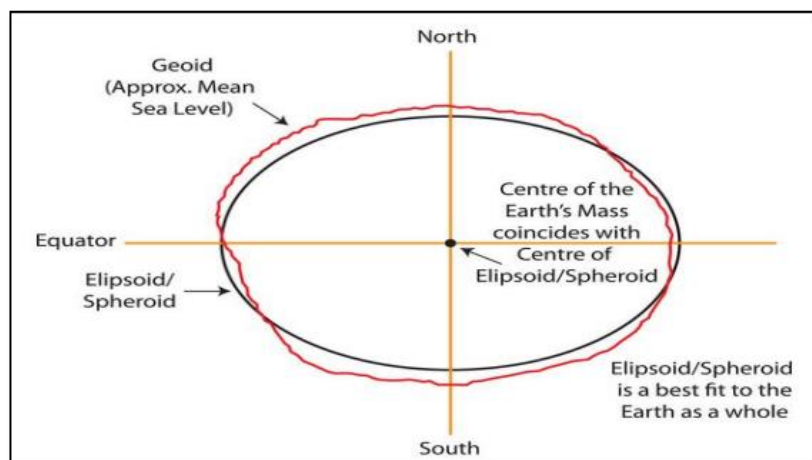


Figure 3.4 Geocentric Datum (Dakhil, 2015)

3.2.4 Non-Geocentric (Local) Datum

A local datum is defined by the International Federation of Surveyors as a datum that closely estimate the form and size of a specific section of the Earth's sea-level surface. It specifies a reference ellipsoid, the spatial location (coordinates) of an initial station and a direction (azimuth) from that station (Anon., 2014). Its ellipsoidal centre will never line up with the Earth's centre of mass and its z-axis is not parallel to the earth's rotational axis. Majority of the geodetic infrastructures established by countries were based on local datum until quite recently. Geocentric datums are used by Satellite Systems for spatial positioning. The Global satellite System used by the American Satellite system adopts the geocentric datum. A local datum is shown in Figure 3.5.

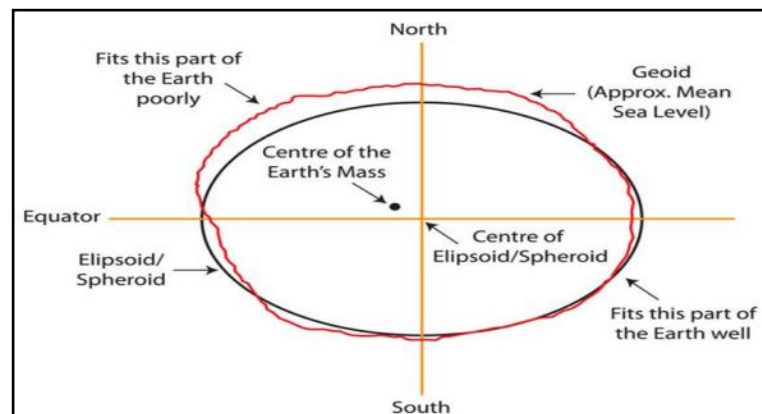


Figure 3.5 A Local Datum (Dakhil, 2015)

3.3 Coordinate System in Geodesy

Points are very essential to Geoscientists as well as geospatial data users. From a geometrical perspective, a point is dimensionless and is designated by an order set of coordinates. Coordinates can be 1D (Height), 2D (Northing and Easting), or 3D (φ, λ, h) or (X, Y, Z) . A coordinate system is described as a collection of numbers that specifically identify a point's location in space. To determine points attributes in space and depict them on maps, one must understand the principles of coordinate systems. A coordinate system describing how coordinates are to be allocated to points, must be established to accurately represent the geographic location of features on a map (Ziggah *et al.*, 2017).

There are many coordinate system in use by geoscientists, but the most common used ones are:

- Geodetic (ellipsoidal) coordinate system
- Geocentric (Cartesian) coordinate system
- GNSS Coordinate System

3.3.1 Geodetic (Ellipsoidal) Coordinate System

A geodetic coordinate system is a coordinate system that indicates the location of objects on the earth's surface based on the angle from the Greenwich meridian known as longitude, the angle from the equator known as latitude, and the height from the ellipsoidal surface of the meridian known as altitude (Eren and Hajiyeve, 2013). This system is extremely accurate when it comes to locating an object near the Earth-space border. It is a three-dimensional coordinate system upon which all mapping systems are based, and it is widely used to store, organize, and communicate geographical data. Figure 3.6 shows the geodetic coordinate system.

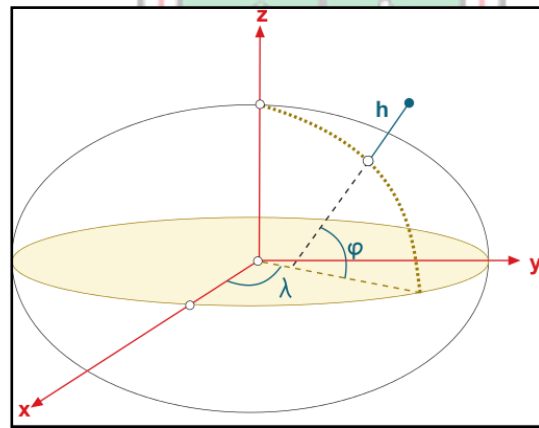


Figure 3.6 Geodetic Coordinate System (Subirana *et al.*, 2011)

3.3.2 Geocentric (Cartesian) Coordinate System

The Geocentric coordinate system refers to the Cartesian coordinate system with 3-dimensions, (X, Y, Z); where Z axis runs parallel to the earth's rotational axis northwards, The X axis runs across the intersection of the prime meridian and the equator, and the Y axis passing via the equator's junction with longitude 90°E the geodetic and geocentric

systems are based on the same geodetic datum (Anon., 2022). For a specific geodetic datum, you find both geodetic and cartesian coordinate systems. Figure 3.7 gives a graphical definition of the Geocentric coordinate system.

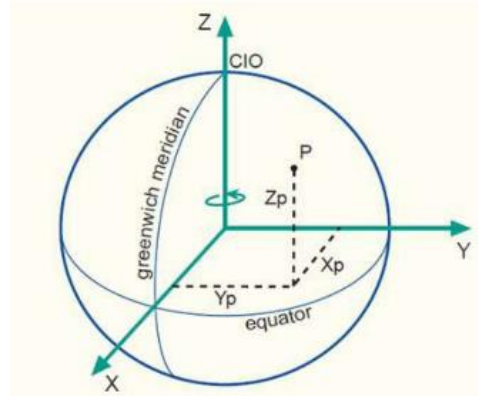


Figure 3.7 Geocentric Coordinate System (Eren and Hajiyev, 2013)

3.3.3 GNSS Coordinate System

The World Geodetic System (WGS 84) is a universal coordinate system. This system is known as the earth-fixed Cartesian coordinates system. Definition of the origin and axis by Hassan *et al.*, (2020) have the following description:

- Its origin coincides with the centre of mass;
- The X-axis is the intersection of the WGS84 reference meridian plane and the plane of the Conventional Terrestrial Pole (CTP) equator.
- Y-axis completes a right-hand, earth-centred earth-fixed (ECEF) orthogonal coordinates system measured in the plane of CTP equator 90° east of the X-axis
- the Z-axis is aligned parallel to the direction of the CTP for polar motion as initially defined by the Bureau International de l'Heure (BIH) and in 1989 by the International Earth Rotation Service.

The WGS 84 is a global coordinate system used by the GNSS-GPS and thus, provides a single, common, accessible three-dimensional coordinate system for geospatial data collection. Positions can be defined as X, Y, and Z or geographic coordinates of latitude, longitude and ellipsoidal height respectively. This system is graphically depicted in Figure 3.8.

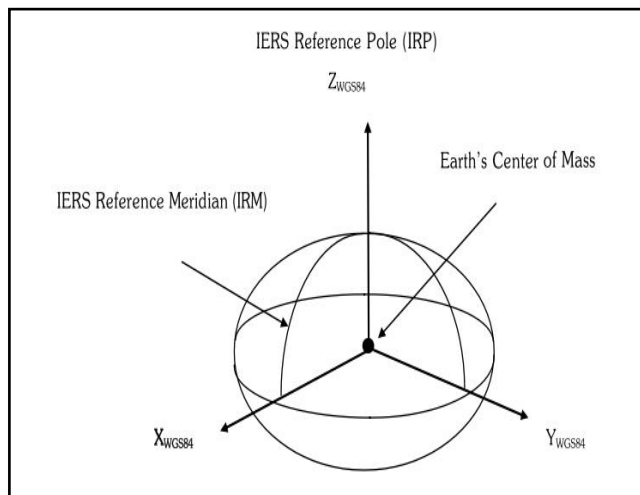


Figure 3.8 The WGS 84 Coordinate System (Boon and Setan, 2007)

3.4 Coordinate Conversion

The process of changing a coordinates system to another coordinate system is known as coordinate operation. A coordinate operation can be within the same datum or from one datum to another datum. Operation within the same datum is called Coordinate conversion.

Conversion of coordinate can be termed as:

- Forward Conversion (geodetic to cartesian); and
- Reverse Conversion (Cartesian to geodetic)

3.4.1 Forward Conversion

Forward conversion is a coordinate operation within the same datum that changes the geodetic coordinate (θ, λ, h) to the cartesian coordinate (X, Y, Z) . This is the first step in coordinate transformation. A straight and easy to follow conversion of the geodetic coordinates (θ, λ, h) above a reference ellipsoid to the cartesian coordinates (X, Y, Z) could be carried out using the Bowring forward equation.

3.4.2 Reverse Conversion

The reverse conversion is simply transferring cartesian coordinates back to the geodetic coordinate of the same system. This is done to enable the coordinates to be projected onto the transverse Mercator. There is a clear and easy to follow relation that exists between the Universal Transverse Mercator (UTM) projected coordinates and the geodetic coordinates.

3.5 Coordinate Transformation

Currently, the principal method for collecting geospatial information is the Global Navigation Satellite System (GNSS), which includes the Global Positioning System that is based on the WGS84. It is necessary to perform coordinate transformation in order to localize the GPS-derived datasets. The transformation of coordinates from one reference frame to another reference frame is a problem in spatial data processing (Ziggah and Yukubu, 2017). Coordinate transformation is defined as a mathematical approach that enables one to transfer coordinates of point from datum I to datum II and vice versa within the same geographic area (Ziggah and Laari, 2018).

Coordinate transformations are used to bring spatial data into a common reference system. Most nations have established their universal frame of reference. For instance, since the GNSS-GPS, which uses the WGS 84 datum, is the extensively utilized instrument used for data collection, spatial data relating to the WGS 84 system must be transformed to the Local system so the data can be integrated into the local system. The Geocentric model, Abridge Molodensky model, Molodensky-Badekas model, Bursa-wolf model, Veis model are only a few of the three-dimensional (3D) conformal transformation models that can be used to transfer coordinates from one system of a datum to another. Factors that influence which model should be used include:

- ✓ The size of the area.
- ✓ The Magnitude of the distortion in both networks.
- ✓ The Nature of the network; 1D, 2D or 3D.
- ✓ The accuracy required.

Since datum transformation had become so paramount because of the local datum adopted by countries, geodesists had categorized coordinate transformation into two as:

- ✓ 2D transformation
- ✓ 3D transformation

The focus of this study is on the 3D transformation.

3.5.1 Three-Dimensional Transformation

The 3D transformation model considers the X, Y, and Z axes in its formulation. A 3D transformation model has seven parameters that defines a functional relationship of coordinates in the two systems. These parameters include: three origin shift parameters (ΔX , ΔY , ΔZ) responsible to make the two origins to coincide, three rotation parameters (R_x , R_y , R_z) responsible to make the two-system axis parallel in all direction, and one scale parameter (sf) to account for any difference in scale between the two systems (Solomon, 2013).

Bursa – Wolf Model

The 3D conformal coordinate transformation also known as the 3D similarity Model is widely used for geodetic applications by surveying, photogrammetry, and geodesy professionals (Ziggah, 2022). The Bursa-Wolf model has seven-parameters which include: scale change, three axes' rotations and three origin- shifts to relates points in two different 3D coordinate system (Ziggah *et al.*, 2016a). The geometry of Bursa-Wolf model is presented in Figure 3.9

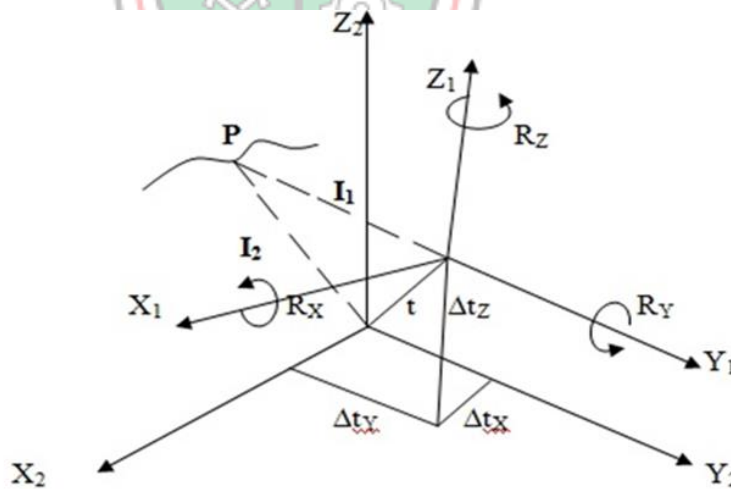


Figure 3.9 Geometry of Bursa-Wolf Transformation (Deakin, 2006a)

The Bursa – Wolf Transformation model Equation (3.2) is expressed in vector form as

$$I_2 = t_2 + (1 + ds)R_s I_1 \quad (3.2)$$

this can be also expressed in matrix form Equation (3.3) as:

$$\begin{bmatrix} X \\ Y \\ Z \end{bmatrix}_2 = (1 + \Delta S) \begin{bmatrix} 1 & R_Z & -R_Y \\ -R_Z & 1 & R_X \\ R_Y & -R_X & 1 \end{bmatrix} \begin{bmatrix} X \\ Y \\ Z \end{bmatrix}_1 + \begin{bmatrix} t_X \\ t_Y \\ t_Z \end{bmatrix} \quad (3.3)$$

3.5.2 Artificial Intelligence

One of the most recent scientific and engineering disciplines is AI. After World War II, work began; and the name was first used in 1956 (Russell and Norvig, 2010). AI is of two words, Artificial, which means man-made and intelligence, means thinking power. Based on these two words, AI can be referred to as man-made thinking power.

However, AI is an aspect of computer science that deals with the development of computers or machines that are as intelligent as humans. AI studies how the human brain works, how we learn, how we make judgement and how we solve real world problems (Shirkin, 2020); a technology which tries to mimic how the human being reasons, how animal reasons, how the trees reason, how we stay in our environment, how the trees mate to produce their offspring, all comes into AI.

AI approaches are universal function approximation; they are applied in many disciplines such as biology, computer science, mathematics, Statistics, geosciences and etc. AI is an umbrella that covers Machine Learning (ML) and deep learning. However, to analyse data and learn from the input data, machine learning employs algorithms. There are three main types of ML: supervise Learning, unsupervised Learning and reinforced supervise learning.

Artificial Neural Network (ANN)

Based on our understanding of how the human brain responds to stimuli from sensory inputs, ANN that depicts the relationship between an input and an output signal (Lantz, 2013). To solve issues, the ANN employs a network of artificial neurons, similar to how the brain employs a network of interconnected cells known as neurons to build a massively parallel processor. As a result, ANNs are motivated by the human being's occupational functionality and its capability of investigating and processing data to produce optimal results employing a network of interconnected artificial neurons. (Dutta *et al.*, 2010). The following are the components of a mammalian neuron's basic structure: nucleus, cell body, dendrites, synapses or synaptic terminals and axon (Figure 3.10) which is artificially represented as (artificial neurons) in (Figure 3.10) as inputs (dendrites), interconnections

(synapses), node which is summing junction of the inputs, weight and bias (cell body) and the output (axon). The strength of AI is its ability to handle both linear and non-linear data; linear and non-linear regression problems.

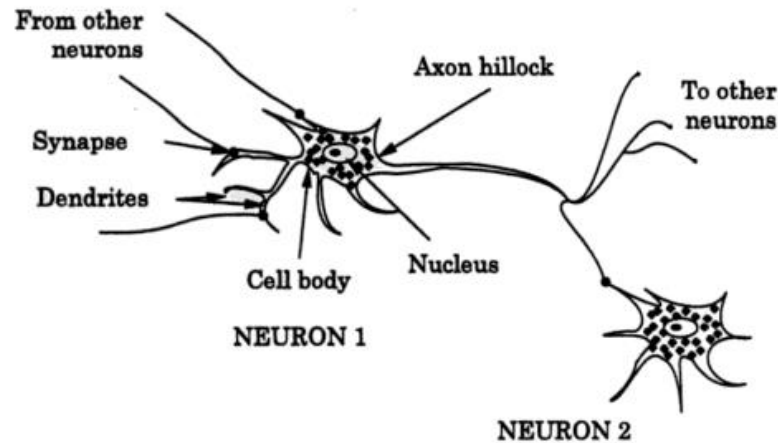


Figure 3.10 A Schematic Diagram of a Biological Neuron (Yegnanarayana, 2005)

Group Method of Data Handling

The Group Method of Data Handling (GMDH), a learning technique inspired by nature, uses polynomial transfer functions to generate a nonlinear mapping of consecutive neuron layers to approximate the relationship between inputs and outputs (Amiri and Soleimani, 2021). This technique is useful for approximating function, recognising patterns, and identifying higher order non-linear systems (Kumi-Boateng and Ziggah, 2020b). Ivakhnenko designed the GMDH with the goal of reducing the difficulties involved with identifying system variables, that was required in other models but usually difficult to calculate (Ivakhnenko, 1971). Therefore, geoscience professional usually estimate the variable which are time consuming and unreliable predicted outcome. Hence, the GMDH became evolved to conquer such issues via its self-setting up nature (AlBinHassan and Wang, 2011). The GMDH is made up of a feed-forward multilayer network (Figure 3.11) of quadratic neurons to represent the functional connection between the input-output variables (Kumi-Boateng and Ziggah, 2020b).

The technique is known for its excellent prediction capabilities, speed in learning, and ability to convert to the best regression surface. This occurrence is possible as a result of the GMDH's optimization strategy, which regularly chooses the best shape by employing a pruning process in a layer-by-layer manner relying on the mean squared error (MSE) criterion (Assaleh *et al.*, 2013). The system will automatically cease adding layers if the MSE of the next layer is greater than the MSE of the previous layer. In this case, the algorithm chooses the low MSE component in the top layer as its final model result (Kumi-Boateng and Ziggah, 2020b).

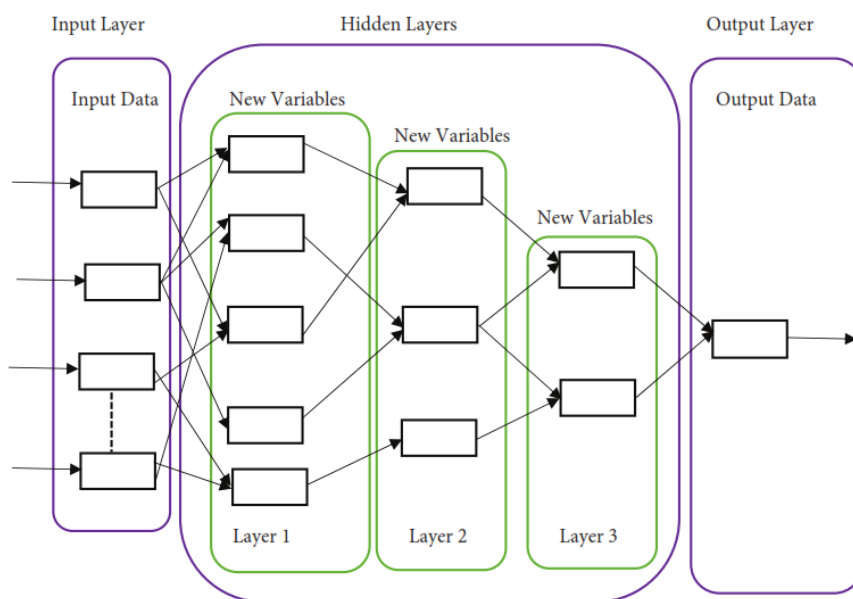


Figure 3.11 Basic GMDH Structure (Kumi-Boateng and Ziggah, 2020b)

Least Square Support Vector Machine

The Least Square Support Vector Machine (LS-SVM) is the least squares formulation of Support Vector Machine employed to provide solution to classification and function estimation related problems (Suykens *et al.*, 2022). The LS-SVM used for this research was designed as a function approximator to perform coordinate transformation. The design involves solving a set of linear equations to find the model parameters. Given a model building data, $D = \{(x_m, y_m) | m = 1, 2, \dots, n\}$ with input data $x_m \in R^t$ and its corresponding output $y_m \in r$, where R^t is the t - vector space dimension and r the one-dimensional vector space. The rationale is to fit a functional model $y(x)$ on the model building data such that the model becomes useful to infer the y target for a new input data

point r . The LS-SVM model is mathematically given by (Ziggah *et al.*, 2019a) in Equation (3.4):

$$y(x) = w^T \phi(x) + b \quad (3.4)$$

Where, w is the adjustable weighted vector; T , the transpose; $\phi(x)$, the non-linear transformation that maps the input data into a higher dimensional space and b is the scalar threshold. Considering the structural Risk minimization rule, Equation 2.1 gives the LS-SVM function approximation model for transforming coordinates (Ziggah *et al.*, 2019a).

3.6 Map Projection

A map projection is a methodical conversion of a position's latitude and longitude on the surface of the Earth to a piece of paper (Ghaderpour, 2015). Specifically, a map projection is the process of converting a set of geodetic coordinates (the latitude and longitude) into a set of plane coordinates on a map (the Cartesian coordinates x and y); such that: (Lat, Long) = (Y, X) or (N, E). Mapmakers attempt to convert the earth, a spherical, round globe, to flat paper. Cartographers use map projections to provide a spherical globe on a plane. When going from a curved surface to a plane, angles, areas, directions, and distances might deform. However, distortion occurs whenever the Earth's surface is converted to a flat surface, and no map projection is flawless. Whether the earth is a sphere or a spheroid, its surface cannot be precisely developed into a plane, just as it is not possible to completely flatten a peel of an orange without shattering it. As a result, whatever method is employed to display a big area on a map, there will always be some deformation. Due to this, unlimited map projections have been developed for mapmaking (Solomon, 2013). Each map projection keeps certain spatial characteristics while losing others.

Cartographer classified map projections based on property preserved (conformal, equal area, equal distance and azimuthal projections), Projection surface (Conical, cylindrical and Planar), geometrical (Gnomonic, stereographic, orthographic projections) or mathematical (Mercator projector), Aspect (Normal, transverse and oblique) and the relationship between the projection surface and the globe (tangent projection and Secant Projection) (Usery *et al.*, 2020). The conical, cylindrical and azimuthal projections are the three major projection classes that are named after the developable surface (Delmelle and Dezzani, 2015). They have linear or point contact with the sphere.

The advantage of these shapes is that, their curvature is in one dimension only, they can be flattened to a plane without any further distortion (Delmelle and Dezzani, 2015). Some projection surfaces are shown in Figure 3.12.

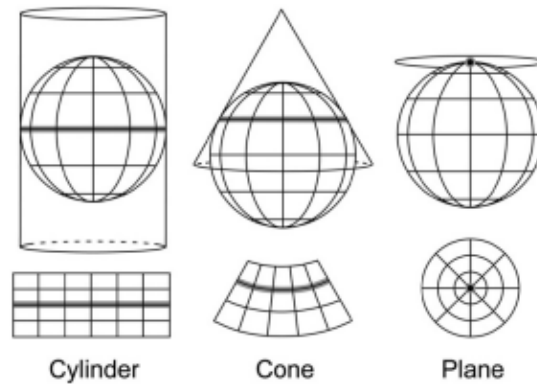


Figure 3.12 Projection Surfaces of Map Projection (Usery *et al.*, 2020)

The scale factor of the projection and the map scale are two frequently misunderstood map projection-related numbers. In contrast to a map scale, which is an approximation for converting map distances to terrestrial distances and is typically printed on the map, a scale factor of the projection is used to calculate precise direction and distance using a map projection's coordinates. It is calculated as the ratio of the length of an arc along a differentially small line in the projection plane to the length of an arc on the ellipsoid.

3.6.1 Mercator Projection

The point scale factor for the Mercator projection is one along the equator, and it is a cylindrical, conformal projection. The equator is known as the line $y = 0$. At the poles, this projection is vague. Mercator developed it in 1569 as a result of his attempts to make the loxodrome, also known as the line of constant bearing on the globe, appear as a straight line on the map (Usery *et al.*, 2020). Meridians and parallels are straight lines forming a rectangular grid. Meridians are equidistantly spaced; parallels are spaced at distances increasing rapidly away from the equator. To produce a true conformal projection, Mercator introduced exactly the right degree of north-south increase in scale needed to match the east-west increase in scale resulting from maintaining parallel meridians. Thus, at 60° , the east-west scale has been increased to twice that at the equator (Gomes and Hut, 2019). Thus, true scale is only at the equator. Meridians are vertical straight lines with equal spacing, while

parallels are horizontal lines with variable spacing (Usery *et al.*, 2020). In this projection, the poles are at infinity on the map, therefore the parallel spacing gets wider as you get closer to them. The Mercator projection is unique in that, in addition to conformity, the rhumb line of the earth is depicted on the map as a straight line, making it extremely useful for navigation.

3.6.2 Transverse Mercator Projection

A transverse Mercator projection is a normal Mercator projection that has been rotated via a 90° angle so that it is related to a central meridian similarly to how a regular Mercator projection is related to the equator (Usery *et al.*, 2020). The scale is accurate along a meridian known as the central meridian because the cylinder is tangent to the globe at that point. This projection is conformal, just like the standard Mercator, however it loses the Mercator's ability to project straight lines. A cylindrical transverse Mercator projection is presented in Figure 3.13.

The projection further characteristics include:

- a straight line is used to symbolize the centre meridian and a line perpendicular to it;
- parallels are complicated curves that are concave toward the pole, while other meridians are complicated curves that are concave toward the 0° longitude; and
- only along the centre meridian is the scale accurate.

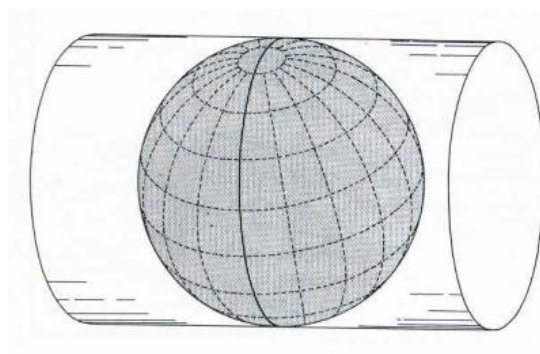


Figure 3.13 Cylinder Orientation for the Transverse Mercator Projection (Gomes and Hut, 2019)

3.6.3 Universal Transverse Mercator Projection (UTM)

The Universal Transverse Mercator (UTM) offers global georeferencing with high degrees of accuracy; it is an extension to Transverse Mercator (TM) projection system, formulated in 1936 by the International Union of Geodesy and Geophysics and later adopted by the US Army in 1947 (Ziggah, 2017). UTM coordinates define two dimensional horizontal positions. An equiangular transverse secant cylindrical projection is how the UTM projection can be conceptualized physically.

There is a Sixty zone numbering system of the Universal Transverse Mercator projection labelled from one to sixty, starts at one hundred eighty degrees West longitude and ends at one hundred eighty degrees East longitude (Deakin, 2006b). The central meridian is placed in the middle of each zone, with three degrees on both sides of the central meridian. Additionally, this projection technique places the true origin of coordinates for each zone at the point where the equator and the central meridian intersect, with a central meridian scale factor of 0.9996 (Deakin, 2006b). Each zone is further subdivided into strips of eight degrees latitude starting at eighty degrees S. The letters C through X are assigned, while O and I are left out in order to prevent distortion. In order to prevent negative coordinates, each zone is assigned a false Easting and a false Northing coordinate that are placed 500 000 meters west of the true origin for the northern hemisphere and 50 000 meters west and 10 000 000 meters south of the true origin for the southern hemisphere, respectively (Deakin, 2006b).

3.6.4 Geography Coordinates to Projected Coordinates

Projecting geographic coordinates for the curve earth surface to a plane (map) and vice versa is done with the help of mathematical models. This research presents the models for moving from geodetic coordinates to UTM projected coordinate as seen in Equations (3.5) and (3.6).

$$m = a(A_0\theta - A_2\sin 2\theta + A_4\sin 4\theta - A_6\sin 6\theta)$$

$$A_0 = 1 - (e^2/4) - (3e^4/64) - (5e^6/256)$$

$$A_2 = 3/8(e^2 + e^4/4 + 15e^6/128)$$

$$A_4 = 15/156(e^4 + 3e^6/4)$$

$$A_6 = 35e^6/3072$$

m_o is obtained by evaluating in using θ_o

$$v = a/(1 - e^2 \sin^2 \theta)^{1/2}$$

$$\rho = a(1 - e^2)/(1 - e^2 \sin^2 \theta)^{3/2}$$

$$\psi = v/\rho$$

$$t = \tan \theta$$

$$\omega = \lambda - \lambda_o$$

$$N = N_o + k_o(m - m_o + \text{Term 1} + \text{Term 2} + \text{Term 3} + \text{Term 4}) \quad (3.5)$$

Where:

$$\text{Term 1} = \omega^2/2(v \sin \theta \cos \theta)$$

$$\text{Term 2} = \omega^4/24(v \sin \theta \cos^3 \theta (4\psi^2 + \psi + t^2))$$

$$\text{Term 3} = \omega^6/[v \sin \theta \cos^5 \theta (8\psi^4(11 - 24t^2) - 28\psi^3(1 - 6t^2) + \psi^2(1 - 32t^2) - \psi(2t^2) + t^4)]$$

$$\text{Term 4} = \omega^6/40320 [v \sin \theta \cos^7 \theta (1385 - 3111t^2 + 543t^4 - t^6)]$$

$$E = E_o + K_o V \omega \cos \theta (1 + \text{Term 5} + \text{Term 6} + \text{Term 7}) \quad (3.6)$$

and

$$\text{Term 5} = \omega^2/6(\cos^2 \theta (\psi - t^2))$$

$$\text{Term 6} = \omega^4/120[\theta(4\psi^3(1 - 6t^2) + \psi^2(1 + 8t^2) - t^2(\psi^2 + t^2))]$$

$$\text{Term 7} = \omega^6/5040[\cos^6 \theta (61 - 479t^2 + 179t^4 - t^6)]$$

3.7 Review of Application of Artificial Intelligence in Coordinate Transformation

The strength of AI is clearly spelt out and recorded in literatures. It had been applied in the geodetic sector of Ghana and other countries for coordinate transformation. Ziggah *et al.*, (2016b) assessed the performance of the Back Propagation Neuron Network (BPNN), Radial Basis Function Neural Network (RBFNN) and Multiple Linear Regression (MLR) for converting coordinates; a study that was conducted on Ghana's geodetic reference frame. These AI approaches followed the supervised learning technique. The findings indicated that the AI models performed satisfactory prediction of the cartesian coordinates with maximum three-dimension position error of 0.004, 0.011 and 0.627 for the RBFNN, MLR and the BPNN respectively.

Ziggah *et al.*, (2016c) compared the performance of the RBFNN and BPNN in terms of plane coordinate transformation to that of the conventional (four parameters and six parameters) models. This paper was the first to transform plane coordinates between the Accra and Legon datums. In the past, the tradition transformation methods have been an aid to geospatial data users. Nowadays, the ANN has been recommended for coordinate transformation because of its power to absorb the heterogeneities and deformation existing in Ghana's two datums. The results showed that the RBFNN performs better than the BPNN and the classical methods when transforming plane coordinates from Legon datum to Accra datum; however, when transforming the same plane coordinate from Accra to Legon datum, both the RBFNN and BPNN are nearly identical but perform better than the classical methods. The study's key contribution was to assess and evaluate ANN's usefulness as a tool for transforming plane coordinates between the Accra and Legon datums. It was concluded that ANN can be used for practical surveying activities

The Geocentric Translation Model, is not a priority in-terms of model selection for coordinate transformation because of its low accuracy obtain as compare to the others models.

Ziggah *et al.*, (2017) developed, tested and compared a new technique potential enough to strengthen the accuracy of Geocentric Translation Model. The authors used official parameters (OP) and additional parameters found from the arithmetic mean (AM) model to move coordinates from the WGS datum to the Accra datum. With regard to the result, the maximum horizontal position error was not welcoming with the OP and AM values of 2.75

and 1.99 respectively. Interestingly, an Error Compensation Model (ECM) was developed that incorporates the BPNN, RBFNN and the Generalized Regression Neural Network (GRNN) to account for the GTM error relative to the AM parameter. The new model reduced the error by 1.06 m. it was shown clearly that the accuracy of the ECM was far better than the GTM models.

Kumi-Boateng and Ziggah (2017) applied a novel approach, the RBFNN to transform plane coordinates between the Legon 1977 datum and Accra 1929. The RBFNN results were compared with the four-parameters and six-parameters models. The results show that the RBFNN predicted accurate and trusted results than the four-parameter and six-parameter models. The writers spelt out the strength of the RBFNN in handling the distortion associated with the local datum, a task that the classical methods (four-parameter and six-parameter) cannot do. It was concluded that the ANN is a good alternative tool for plane coordinate transformation because of its ability to compensate for the distortion in the local reference networks.

Ziggah *et al.*, (2018) investigated the applicability of the Extreme learning machine (ELM), a new modern approach to coordinate transformation. The ELM model was tested on the Ghana's geodetic network and compared to the BPNN, RBFNN and the 2D Affine and 2D conformal models. The findings indicated that the ELM can deliver a reliable transformation result as compared to the BPNN and RBFNN; the ELM method is preferred because of its lesser computational time. Besides, building the structure of the ELM is easy and direct. On the other hand, ELM performance was superior to 2D affine and 2D conformal models.

In Ziggah *et al.*, (2019a) the Least Square Support Vector Machine (LS-SVM), a coordinate transformation extension of the Support Vector Machine, was studied in 2019a to see how well it performed and how useful it was. The LS-SVM was for the first time tested on the Ghana geodetic reference frame. The writers compared the SVM and the RBFNN, BPNN, 2D conformal and 2D affine transformation models. The RMSE and SD were used to assess the performance of the various models. The findings revealed that the LS-SVM produced comparable results as the RBFNN, but the two models performed better than the other models. It was determined that the LS-SVM should be employed as an alternative technique for transforming coordinates because it satisfies Ghana's cadastral survey's accuracy requirements. The LS-SVM exhibits outstanding predictive power.

Ziggah *et al.*, (2019b) performed coordinate transformation between global and local datum based on artificial neural network using k-fold cross validation technique. This study was the first research to look at the potential of the *K*-fold cross validation method in the performances of the Bursa-Wolf model and radial basis function neural network under sparse data situation in the Accra datum. It was mentioned that the hold-out cross validation has its weakness of inappropriate data partitioning. Bias and large variance may result from incorrect data division. The outcomes demonstrated that inappropriate data division of the sparse dataset for the local geodetic reference network into a single train-test experiment could result in incorrect conclusions that only depend on how the data was divided and the split set selected. The results showed that the RBFNN outperformed the Bursa-Wolf model, with horizontal position errors of 0.797 and 1.188 m, respectively, for the root mean square.

Kumi-Boateng and Ziggah, (2020a) conducted research on the application of the RBFNN and total least square (TLS) for coordinate transformation in Ghana. The primary goal of the authors was to enhance TLS-RBFNN, estimation performance in coordinate transformation. The geodetic reference frame for Ghana was subjected to this hybrid technique. The results showed that the TLS-RBFNN increased the root mean square horizontal residual transformation accuracy of TLS and RBFNN by 20.2% and 37.3%, respectively. The TLS-RBFNN increased the transformation precision by 0.37% and 8.52%, respectively, with respect to the Standard Deviation (SD). In support of this, the Bayesian information criterion (BIC) showed that the hybrid technique is more effective than utilizing the TLS and RBFNN separately. It was seen that the TSL-RBFNN has the ability to modify its learning behavior to learn the complex patterns of the dataset.

Kumi-Boateng and Ziggah (2020b) assessed the effectiveness of coordinate transformation using the GMDH. The spatial position of the used data is in Accra 1929 and Legon 1977 datums. In Kumi-Boateng and Ziggah (2020b), the RBFNN, BPNN, 2D conformal, and 2D affine models were contrasted with the GMDH. The suggested GMDH method converts coordinates from the Legon 1977 datum to the Accra 1929 datum very effectively. Additionally, it was discovered that GMDH can provide comparable and gratifying outcomes compared to those of the well-known BPNN and RBFNN. In comparison to the machine learning models, the classical models underperformed. These authors observed that the self-adaptive ability of machine learning models to identify patterns in a data collection

without taking into account any functional relationships between the input and output variables is credited with the computational strength of these models. Based on the results, the GMDH model has demonstrated interesting application potential for executing coordinate transformation and has broad implications as a supplement approach for the geospatial and built environment practitioners in Ghana.



CHAPTER 4

RESOURCES AND METHODS USED

This chapter gives detail on the materials used for the study as well as the methods and procedures. All computations that were not detailed in the Literature review are been captured here.

4.1 Resources Used

4.1.1 Data Description

The data obtain for this thesis is a secondary data of 34 common points of coordinates (θ, λ, h) for the WGS system and (θ, λ, h) for War Office system; the corresponding projected coordinates (Northing, Easting) were also obtained. These points were observed from thirteen regions by the Survey and Mapping Division of the Land Commission of Ghana. The descriptive statistic of the dataset is given in Table 4.1. Figure 4.1 presents the data distribution.

Table 4.1 Descriptive Statistic of Common Points

	Min	Max	Mean	SD
WGS LONG	-2.8585	0.495148	-1.24893	0.973451
WGS LAT	5.3157	10.88084	7.719204	1.817085
WGS HGHT	51.55	681.632	350.7673	178.1253
WAR LONG	-2.85874	0.494838	-1.24919	0.973426
WAR LAT	5.312912	10.87823	7.716478	1.817148
WAR HGHT	50.99107	680.4475	342.5377	179.3322
NORTHING	234410.9	2253931	1106678	659294.3
EASTING	224631.2	1442408	810291.7	352118.2

WGS LONG, WGS LAT, WGS HGHT, WAR LONG, WAR LAT, WAR HGHT are WGS Longitude, WGS Latitude, WGS Height, WAR OFFICE Longitude, WAR OFFICE Latitude and WAR OFFICE Height.

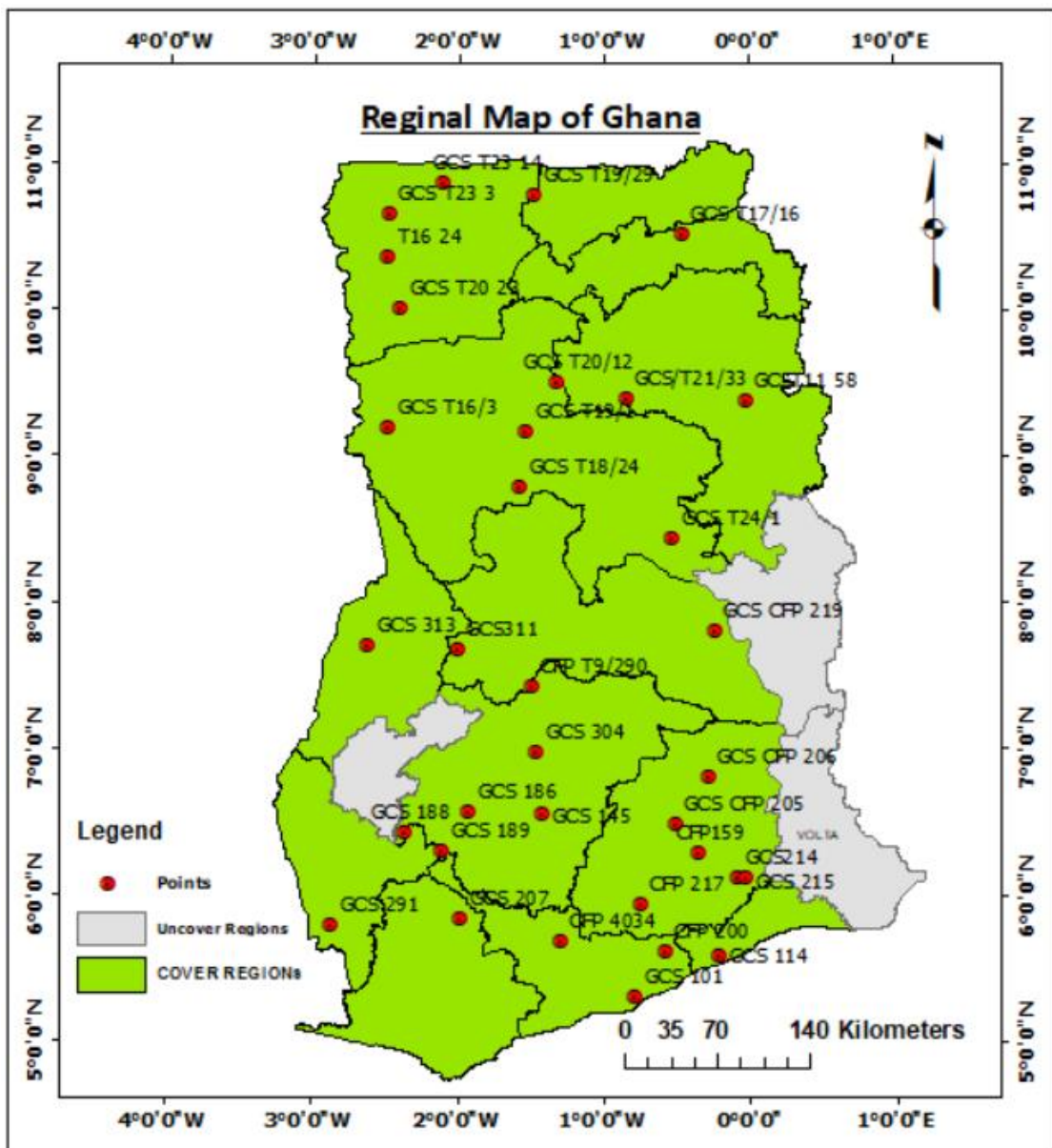


Figure 4.1 Map of Ghana Showing the Research Points

4.2 Method Used

A summary of the various methodologies employed are presented as follows:

- Determining transformation parameters using the Bursa-wolf Model;
- Transforming from $(\theta, \lambda, h)_{wgs}$ to $(\theta, \lambda, h)_{war}$;
- Transformation using AI approach, precisely, the GMDH and the LS-SVM;

- Project the transformed coordinates of Bursa-Wolf as well as the predicted geographic coordinates of the GMDH and the LS-SVM unto the Transverse Mercator used in Ghana.
- Comparison of results, the AI and the classical model.
- Determine the best transformation model based on statistical analysis.

Figure 4.2 presents the flow chart of the coordinate transformation carried out.

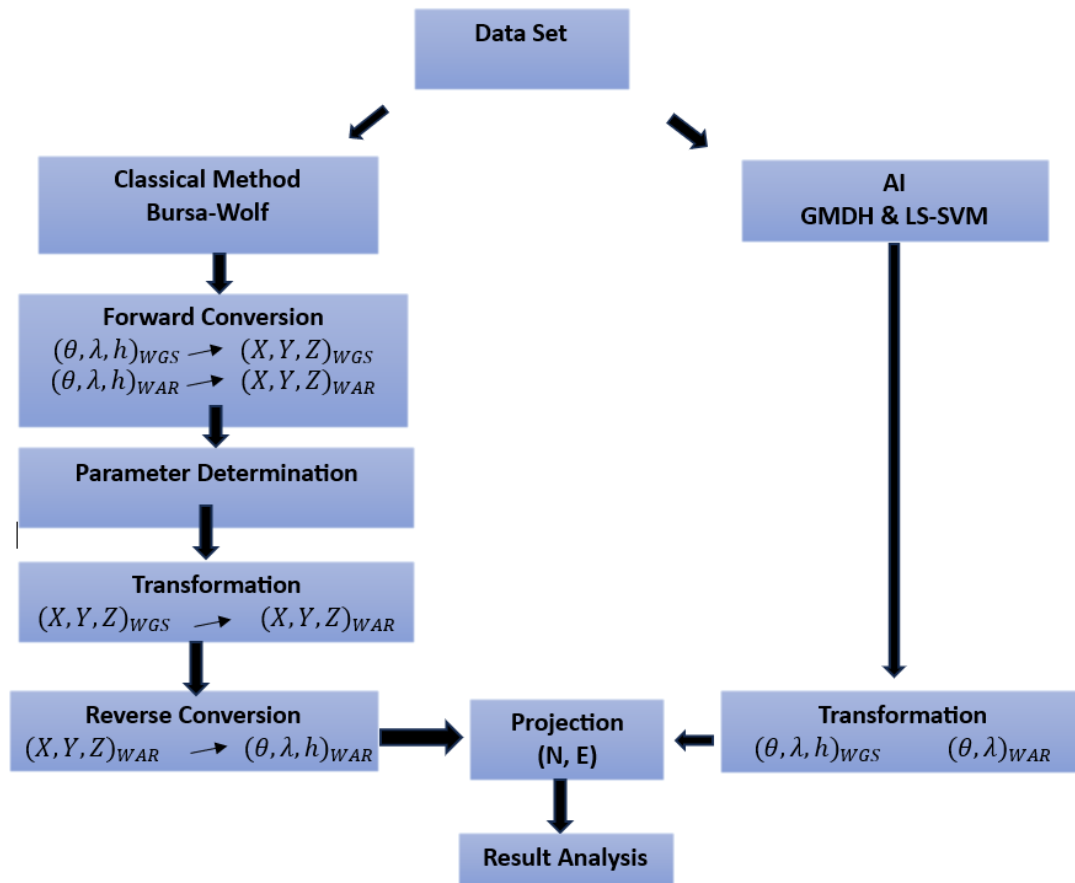


Figure 4.2 The Study's Flow Chart

4.2.1 Forward Conversion Method

Forward conversion was the first step of coordinate transformation when using the 3D seven parameter conformal model of Bursa-Wolf. The geographic coordinates of the WGS84 and the Accra 1929 datums were converted to Cartesian coordinates using the Standard forward equation in Equation (4.1), (Ziggah and Yakubu, 2017). This is because the Bursa-Wolf model utilizes cartesian coordinates.

$$\begin{aligned} X &= (N + h) \cos \Theta \cos \lambda \\ Y &= (N + h) \cos \Theta \sin \lambda \\ Z &= [N (1 - e^2) + h] \sin \Theta \end{aligned} \quad (4.1)$$

where Θ = Latitude, λ = longitude, f = flattening, e = eccentricity. The radius of curvature in the prime vertical plane N , and e^2 the first eccentricity is given by:

$$a/\sqrt{(1 - e^2 \sin^2 \Theta)} \quad (4.2)$$

$$e^2 = f (2 - f) \quad (4.3)$$

4.2.2 Bursa – Wolf Transformation

After the conversion process, the thirty-four points given in the Appendix A were used to determine transformation parameters using the Bursa-wolf model. The ordinary least square technique was applied to the Bursa-Wolf model for determining the transformation parameter. The determined parameters were then used to carry on the transformation from the global to the Accra datum. The least square equation (Laari *et al.*, 2016) is given in Equation (4.4) as

$$AX = V + L \quad (4.4)$$

where

$$X = (A' * A)' * (A' * L)$$

and A is the design matrix, X is the matrix of unknown parameters, L is the observation matrix, and V is the residual matrix. Through Equation (4.5), the seven-parameter transformation model used for this study has relationship with rectangular coordinate (Ziggah *et al.*, 2019b):

$$\begin{bmatrix} X \\ Y \\ Z \end{bmatrix}_{War} = \begin{bmatrix} T_X \\ T_Y \\ T_Z \end{bmatrix} + sR(\alpha_1, \alpha_2, \alpha_3) \begin{bmatrix} X \\ Y \\ Z \end{bmatrix}_{WGS} \quad (4.5)$$

Where, $\begin{bmatrix} X \\ Y \\ Z \end{bmatrix}_{WGS}$ is the WGS coordinate, $\begin{bmatrix} X \\ Y \\ Z \end{bmatrix}_{WAR}$ is the War Office Coordinate, and

$\begin{bmatrix} T_X \\ T_Y \\ T_Z \end{bmatrix}$ are the respective translation parameters along the x , y , and z axis

s is the scale factor

R is the matrix of total rotation given as:

$$R = \begin{bmatrix} \cos\alpha_3 & \sin\alpha_3 & 0 \\ -\sin\alpha_3 & \cos\alpha_3 & 0 \\ 0 & 0 & 1 \end{bmatrix} \begin{bmatrix} \cos\alpha_2 & 0 & -\sin\alpha_2 \\ 0 & 1 & 0 \\ \sin\alpha_2 & 0 & \cos\alpha_2 \end{bmatrix} \begin{bmatrix} 1 & 0 & 0 \\ 0 & \cos\alpha_1 & \sin\alpha_1 \\ 0 & -\sin\alpha_1 & \cos\alpha_1 \end{bmatrix}$$

where $\alpha_1, \alpha_2,$ and α_3 are the angles of rotation around x, y and z - axes. Expanding Equation (4.5) gives Equation (4.6) given as

$$\begin{bmatrix} X \\ Y \\ Z \end{bmatrix}_{WGS} = \begin{bmatrix} T_X \\ T_Y \\ T_Z \end{bmatrix} + \begin{bmatrix} 1 + s\eta & R_Z & -R_Y \\ -R_Z & 1 + \eta & R_X \\ R_Y & -R_X & 1 + s \end{bmatrix} \begin{bmatrix} X \\ Y \\ Z \end{bmatrix}_{WAR} \quad (4.6)$$

As indicated earlier, the unknown parameters were determined using least squares technique.

$$X = \begin{bmatrix} T_X \\ T_Y \\ T_Z \\ R_X \\ R_Y \\ R_Z \\ \eta \end{bmatrix}, \quad A = \begin{bmatrix} 1 & 0 & 0 & 0 & Z_C & Y_C & X_C \\ 0 & 1 & 0 & Z_C & 0 & X_C & Y_C \\ 0 & 0 & 1 & Y_C & X_C & 0 & Z_C \end{bmatrix}, \quad L = \begin{bmatrix} X_W - X_C \\ Y_W - Y_C \\ Z_W - Z_C \end{bmatrix}$$

where X is the transformation parameters, L is the matrix of observation, and A is the design matrix. The estimated transformation parameters were then used to perform transformation and to project the transformed estimated coordinates onto the Traverse Mercator 1° NW used for surveying and mapping works in Ghana.

4.2.3 Reverse Conversion Method

The bowing inverse equation given by (Kumi-Boateng and Ziggah, 2016) in Equation (4.7), (4.8) and (4.9) was used to convert the calculated projected coordinates back to geodetic coordinates:

$$\begin{aligned} \theta &= \text{Tan}^{-1}(Z + be'^2 \sin^3 \psi) / (P - ae^2 \cos^3 \psi) \quad (4.7) \\ \psi &\cong \text{Tan}^{-1}(aZ/bP) \\ P &= (X^2 + Y^2)^{1/2} \\ e^2 &= f(2 - f) \\ e'^2 &= e^2 / (1 - e^2) \end{aligned}$$

Where ψ is the parametric latitude, P is the perpendicular distance from the rotational axis, e is the first eccentricity, e'^2 is the second eccentricity, a is the semi-major axis, b is the semi-minor axis, and X, Y and Z are the cartesian coordinates.

The longitude is given as (Ziggah, 2017):

$$\lambda = \text{Tan}^{-1}(Y/X) \quad (4.8)$$

$$h = [P/\cos\theta] - N \quad (4.9)$$

4.2.4 Group Method of Data Handling

This study applied the GMDH as one of the AI methods. In the GMDH model development, the supervised learning technique was considered. The training and testing datasets were both normalized. Given that the machine learning method utilized weren't scale invariant, this step was crucial. Kumi-Boateng and Ziggah, (2020b) give the normalized equation in Equation (4.10) as:

$$N_i = N_{min} + (N_{max} - N_{min}) * (O_i - O_{min}) / (O_{max} - O_{min}) \quad (4.10)$$

Where N_i is the normalized data, O_i is the recorded coordinates, O_{min} and O_{max} are the lower and upper interval of the recorded coordinates with N_{max} and N_{min} values set at 1 and -1. The GMDH structure contain an input, hidden, and output layer feedforward structure. The first layer of the network was created using the input variables $(\varphi, \lambda, h_w)_{wgs}$ to build the GMDH model. Each succeeding layer then draws input from the layer before. In this instance, the network neurons' interconnectivity is considered automatically during training to enhance the network rather than being stagnant. The number of layers in the network was picked automatically to prevent overfitting, resulting in superior estimation result. These characteristics illustrate the self-organizing nature of the GMDH approach. The $(\varphi, \lambda, h_w)_{wgs}$ was used as an input to predict the $(\varphi, \lambda,)_{war}$ separately. The predicted coordinates were projected unto the Transverse Mercator of Ghana using the classical model defined in Equations (2.10) and (2.11).

4.2.5 Least Square Support Vector Machine

To utilize the Least Square Support Vector Machine for this research, thirty-four points with coordinates in both WGs 84 and Accra 1929 datum were used. The thirty-four points were divided into five-folds. The average of the statistical indicators of all the five folds represents the actual characteristics of the dataset. A MATLAB code that follows the LS-

SVM algorithm was written to predict the geographic coordinates of the Accra 1929 datum using the WGS 84 datum.

The LS-SVM model takes the $(\theta, \lambda, h_w)_{wgs}$ as input quantities and θ, λ as separate output. Both training and testing data were normalized using Equation (4.10).

The training model of the LS-SVM for this research incorporates the Radial Basis function (RBF) as the kernel function. The RBF predicted very well then, the polynomial and linear kernels. The predicted Accra datum coordinates were then projected unto the Transverse Mercator 1° NW using Equation (3.5) and (3.6).

4.2.6 The K-Fold Cross Validation

The K-fold Cross Validation (KCV) technique was used for the data portioning. The thirty-four points were split into five folds such that each can participate in the training process. Fold-1 to fold-4 contain seven points each while fold-5 has six points. The average of all five folds gives the optimal performance of the model. The use of the K-fold Cross Validation is motivated by the weakness of Hold-out Cross Validation (HCV) in an inappropriate data partitioning circumstance. An incorrect data split could result in a large variation and bias in the results obtained. Furthermore, in the case of a sparse dataset, the HCV is ineffective (Ziggah *et al.*, 2019). Table 4.2 gives a summary of the data partition.

Table 4.2 Five Folds Cross Validation Technique Structure

Numbers of points per Fold	First Trial	Second Trial	Third Trial	Forth Trial	Fifth Trial
	Fold 1	Fold 2	Fold 3	Fold 4	Fold 5
7	Testing	Training	Training	Training	Training
7	Training	Testing	Training	Training	Training
7	Training	Training	Testing	Training	Training
7	Training	Training	Training	Testing	Training
6	Training	Training	Training	Training	Testing

4.3 Model Performance

The usefulness of a model depends on how close the model's prediction is, compared to the targeted value. Checking the precision and quality of the transformation outcomes that were

produced, a statistical analysis of the residuals from all models were accessed. The statistical indicators used in this study to determine the model of best performance are in the preceding sub-heading.

4.3.1 Root Mean Square Error

The Root Mean Square Error (RMSE) is a statistical tool that integrates the ideas of bias and standard deviation and is always positive (Ziggah *et al.*, 2019). It is used to measure how much model predictions deviate from actual data in a system. An RMSE value of zero indicates optimal model performance. However, depending on the projected variable's units, the RMSE may really be any value between zero and infinity. Equation (10) was used to estimate the RMSE, which is given as:

$$RMSE = \sqrt{n^{-1} \sum_i^n (T_i - P_i)^2} \quad (4.10)$$

Where RMSE is the Root Mean Square Error in each direction, n is the number of coordinates, T_i and P_i are Targeted and predicted coordinates.

4.3.2 Root Mean Square of the horizontal Position Error

The Root Mean Square Error of the horizontal ($RMSE_{HE}$) was taken into account to calculate the overall uncertainty in the used integrated data. The ($RMSE_{HE}$) is expressed mathematically in Equation (4.11).

$$RMSE_{HE} = \sqrt{(RMSE_E)^2 + (RMSE_N)^2} \quad (4.11)$$

Where $RMSE_{HE}$ is the Root Mean Square Error of the horizontal error, $RMSE_E$ and $RMSE_N$ are the Root Mean Square Error of the eastings and northings.

4.3.3 Horizontal Position Error

By comparing the transformed coordinates to the desired coordinates, the Horizontal Position Error (HE) was calculated to determine the horizontal correctness of the data.

$$HE = \sqrt{((E_T - E_P)^2 + (N_T - N_P)^2)} \quad (4.12)$$

Where HE is the Horizontal Positional Error, E_T and E_P are the targeted and predicted eastings, and N_T and N_P are the targeted and predicted northings.

4.3.4 Standard Deviation

The precision of the anticipated coordinates generated by the model is assessed by the Standard Deviation (SD). This Standard deviation shows the consistency and spread of the residual.

$$SD = \sqrt{(n^{-1} \sum_{i=1}^n (e_i - \bar{e})^2)} \quad (4.13)$$

Where n is the number of coordinates, e_i is the error between the predicted and targeted grid coordinates with \bar{e} as its mean.



CHAPTER 5

RESULTS AND DISCUSSION

After a series of computations involving the thirty-four points, the results are presented and analysed in this chapter.

5.1 Results

5.1.1 Numerical Transformation Model Results

This study applied the Bursa-wolf transformation where seven parameters were determined. The determined parameters are presented in Table 5.1. The individual standard deviations of the determined parameters have also been presented in Table 5.1. In order to understand the dynamics in the residuals produced when the least squares approach was applied to the Bursa-Wolf model, the residual plot given in Figure 5.1 was utilised.

Table 5.2 Transformation Parameter from Bursa-Wolf Model

Parameter and unit	Value
Tx (m)	-147.435572 ± 3.0123
Ty (m)	30.54724145 ± 6.6271
Tz (m)	328.385179 ± 3.5339
Rx (rad)	$-7.20E-06 \pm 4.90E-07$
Ry (rad)	$9.07E-08 \pm 5.55E-07$
Rz (rad)	$-1.12E-06 \pm 1.03E-06$
Sf (rad)	$-7.70E-06 \pm 4.71E-07$

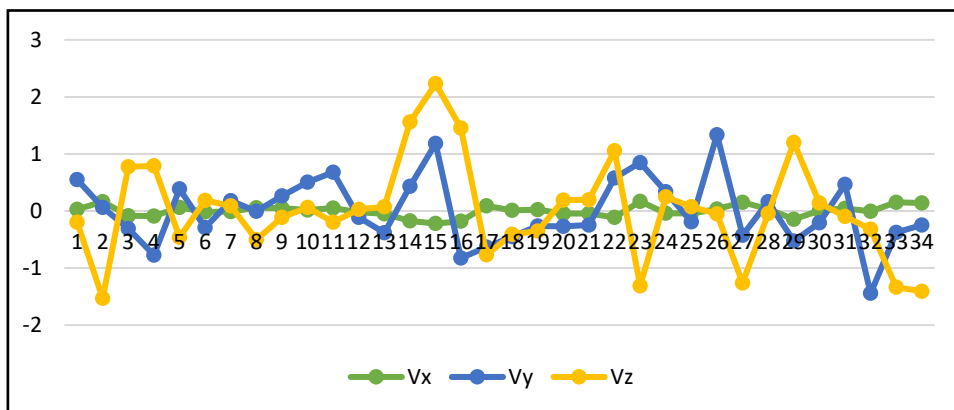


Figure 5.1 Diagram of The Training Residuals of Bursa-Wolf Model

5.1.2 AI Models Developed

In the AI model development, the k-fold cross-validation approach was applied. Here, the 34-data points were divided into five subsets (five folds) where each fold served in the training data. Tables 5.2 and 5.3 present the various k-fold horizontal positional assessments produced by GMDH and LS-SVM. A diagrammatic representation of the performance metrics for each fold is shown in Figures 5.2 to 5.11. the training value has the unit of decimal degree (dd) and the unit of the testing value is meters (m)

Table 5.3 The Horizontal Residual's Performance Metric for Fold 1-3

Statistical Indicator	Fold 1			
	Training		Testing	
	GMDH	LS-SVM	GMDH	LS-SVM
RMSE HE	6.97E-06	6.01E-06	3.294527254	2.65086
Min HE	-1.4E-06	-1E-06	-0.519554739	-0.43282
Max HE	1.57E-05	1.17E-05	8.654837444	6.151843
Mean HE	5.89E-06	5.13E-06	2.658029987	2.257798
SD	5.01E-06	4.29E-06	2.298672148	1.86833
Statistical Indicator	Fold 2			
	Training		Testing	
	GMDH	LS-SVM	GMDH	LS-SVM
RMSE HE	7.98E-06	6.54E-06	2.868324486	2.640839
Min HE	-1.8E-06	-1.8E-06	-0.653631067	-0.48488
Max HE	1.74E-05	1.22E-05	6.302268839	5.305128
Mean HE	7.09E-06	5.85E-06	2.565575293	2.324424
SD	5.7E-06	4.7E-06	2.044930409	1.886544
Statistical Indicator	Fold 3			
	Training		Testing	
	GMDH	LS-SVM	GMDH	LS-SVM
RMSE HE	6.65E-06	5.5E-06	3.253287497	2.688191
Min HE	-1.4E-06	-2.9E-07	-0.518163563	-0.09511
Max HE	1.08E-05	1.06E-05	6.849397678	5.359657
Mean HE	5.96E-06	4.71E-06	2.80429698	2.278811
SD	4.72E-06	3.89E-06	2.27719116	1.866066

Table 5.4 The Horizontal Residual's Performance Metric or Fold 4 and Fold 5

Statistical Indicator	Fold 4			
	Training		Testing	
	GMDH	LS-SVM	GMDH	LS-SVM
RMSE HE	7.48E-06	6.27E-06	2.869958834	2.437454
Min HE	-1.4E-06	-5.3E-07	-0.51592840	-0.20529
Max HE	1.64E-05	1.41E-05	5.972639976	5.128392
Mean HE	6.57E-06	5.44E-06	2.533801251	2.126099
SD	5.32E-06	4.43E-06	2.037204686	1.711717
Statistical Indicator	Fold 5			
	Training		Testing	
	GMDH	LS-SVM	GMDH	LS-SVM
RMSE HE	7.2E-06	5.6E-06	2.869958834	2.35321
Min HE	-1E-06	-1E-06	-0.51592841	-0.4415
Max HE	1.4E-05	1.2E-05	5.972639976	5.09003
Mean HE	6.2E-06	4.7E-06	2.533801251	1.96503
SD	5.2E-06	4.1E-06	2.037204686	1.65959

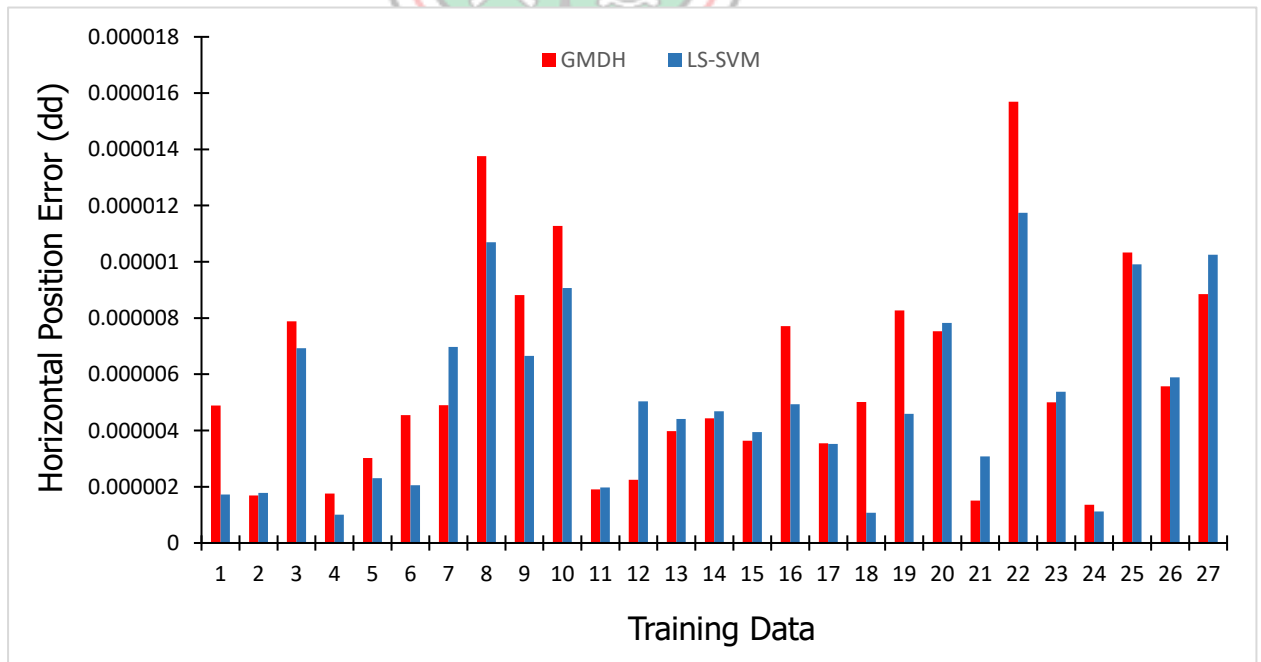


Figure 5.2 Horizontal Position Residuals for Fold 1 (Training)

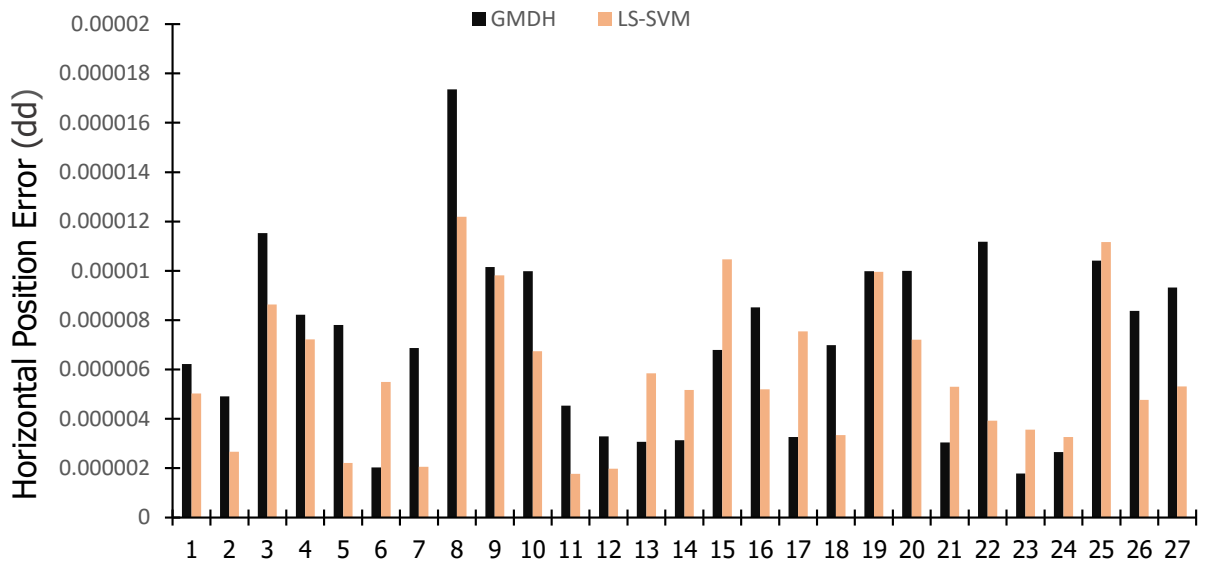


Figure 5.3 Horizontal Position Residuals for Fold 2 (Training)

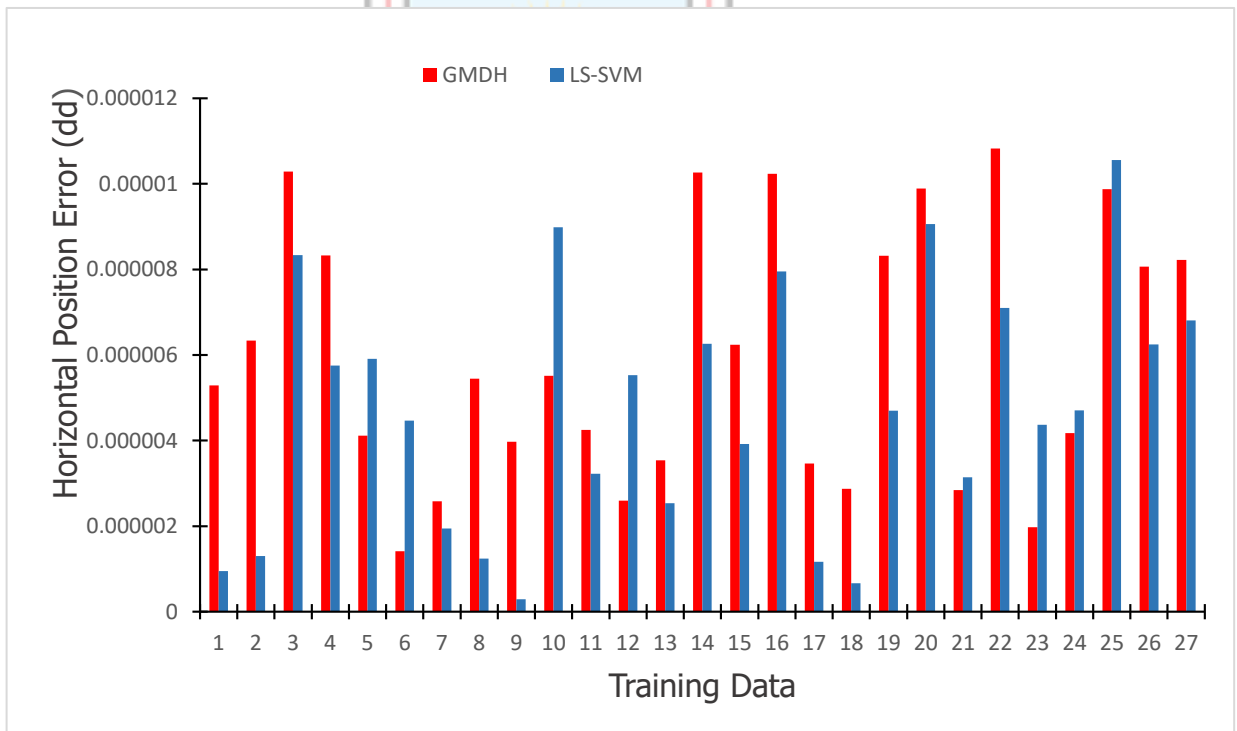


Figure 5.4 Horizontal Position Residuals for Fold 3 (Training)

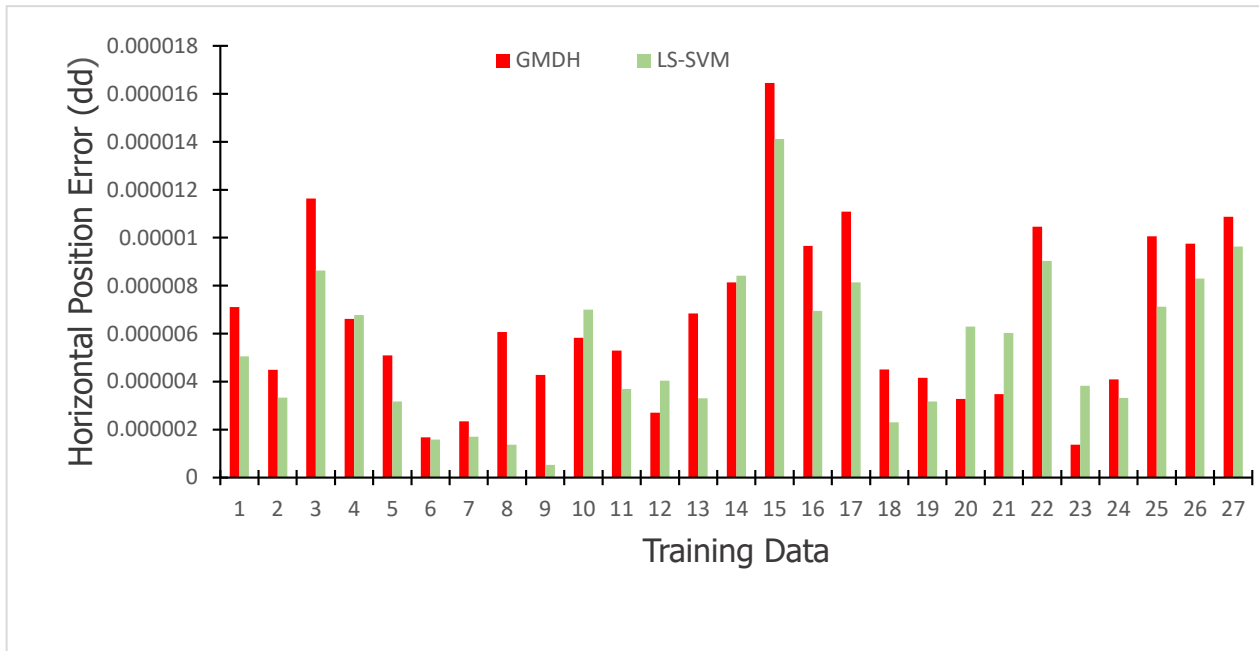


Figure 5.5 Horizontal Position Residuals for Fold 4 (Training)



Figure 5.6 Horizontal Position Residuals for Fold 5 (Training)

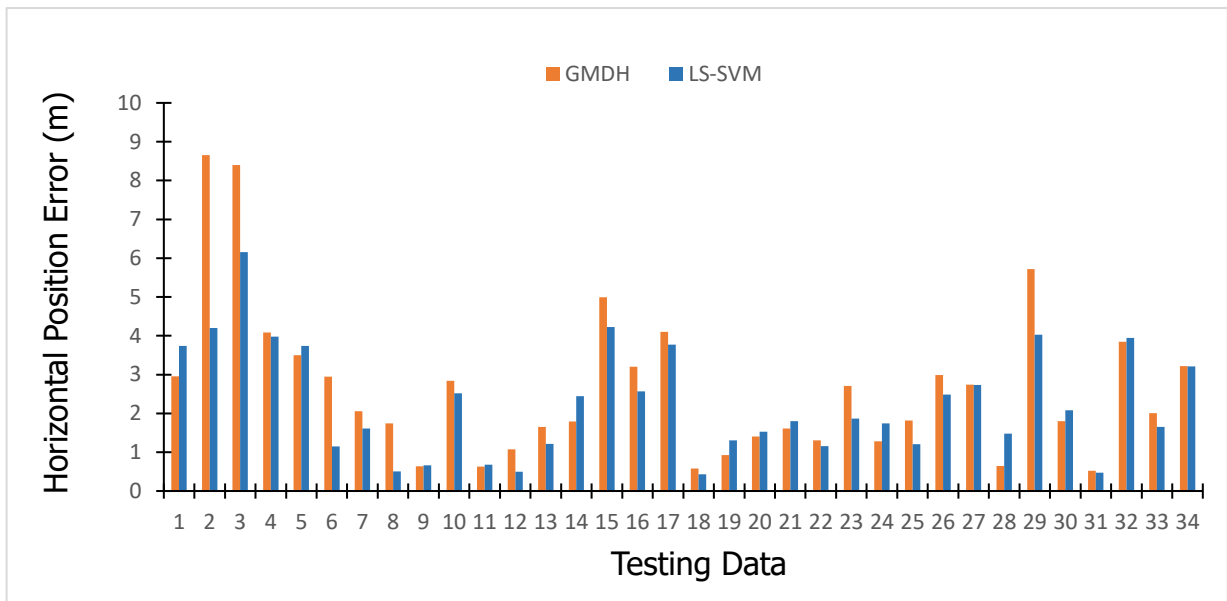


Figure 5.7 Horizontal Position Residuals for Fold 1 (Testing)

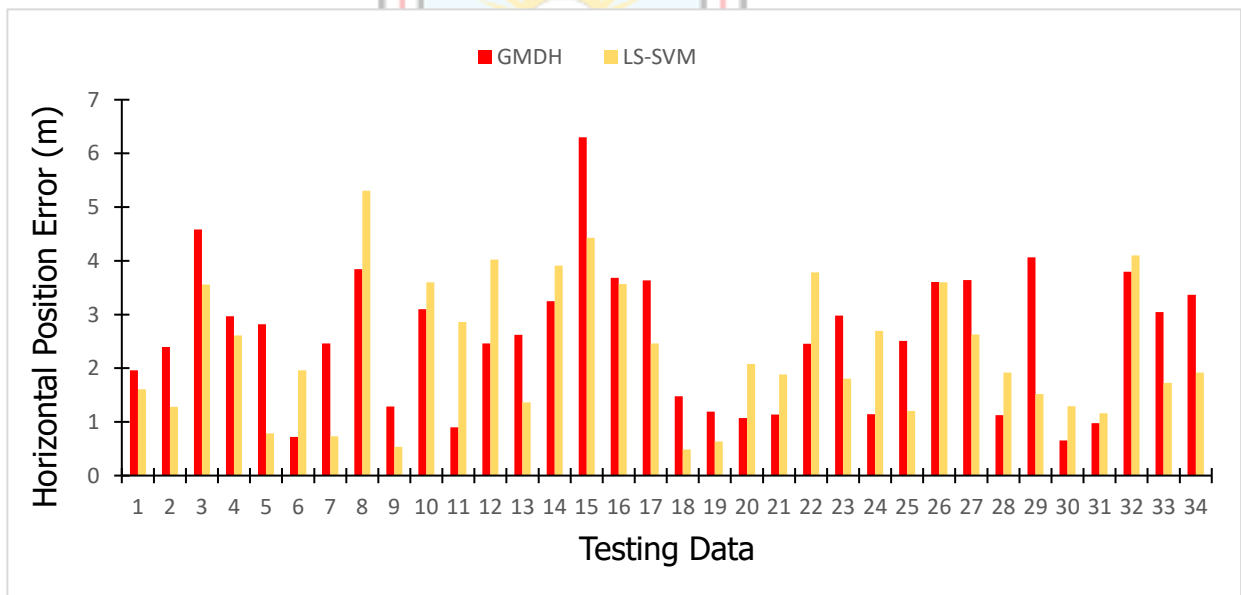
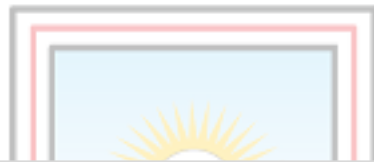


Figure 5.8 Horizontal Position Residuals for Fold 2 (Testing)

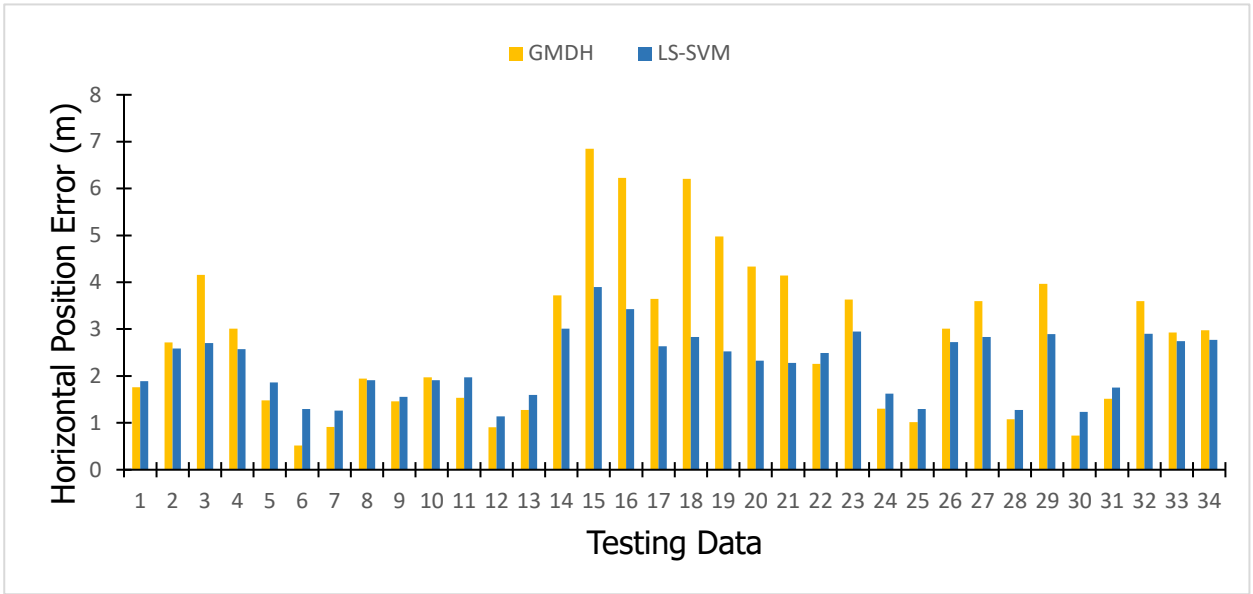


Figure 5.9 Horizontal Position Residuals for Fold 3 (Testing)

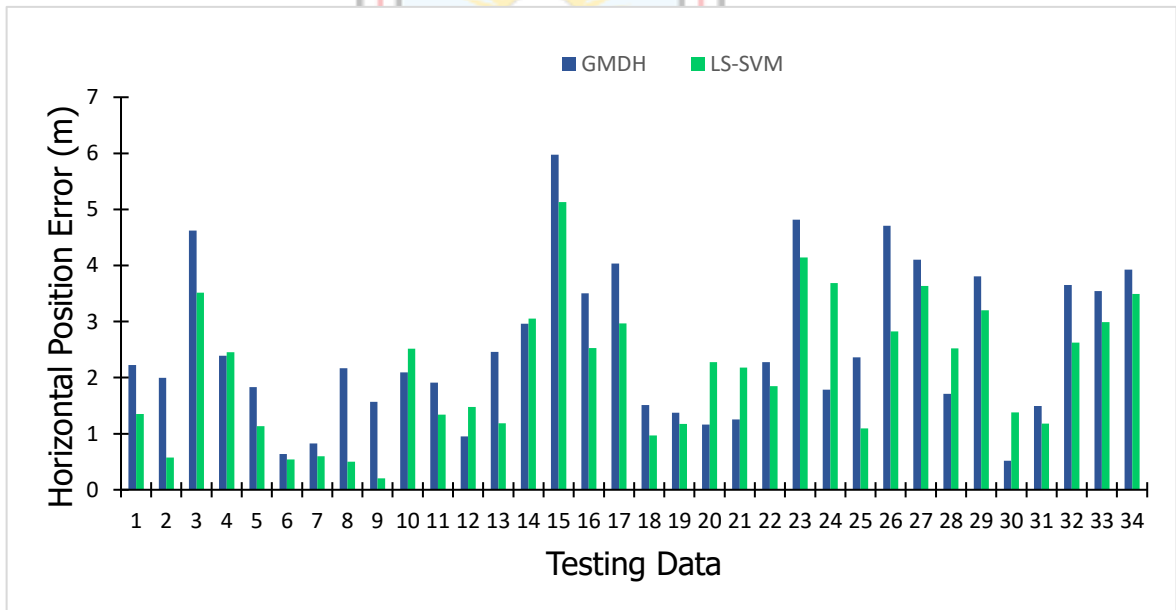
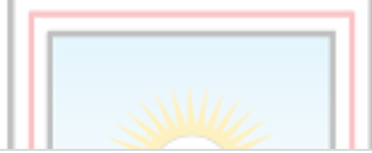


Figure 5.10 Horizontal Position Residuals for Fold 4 (Testing)

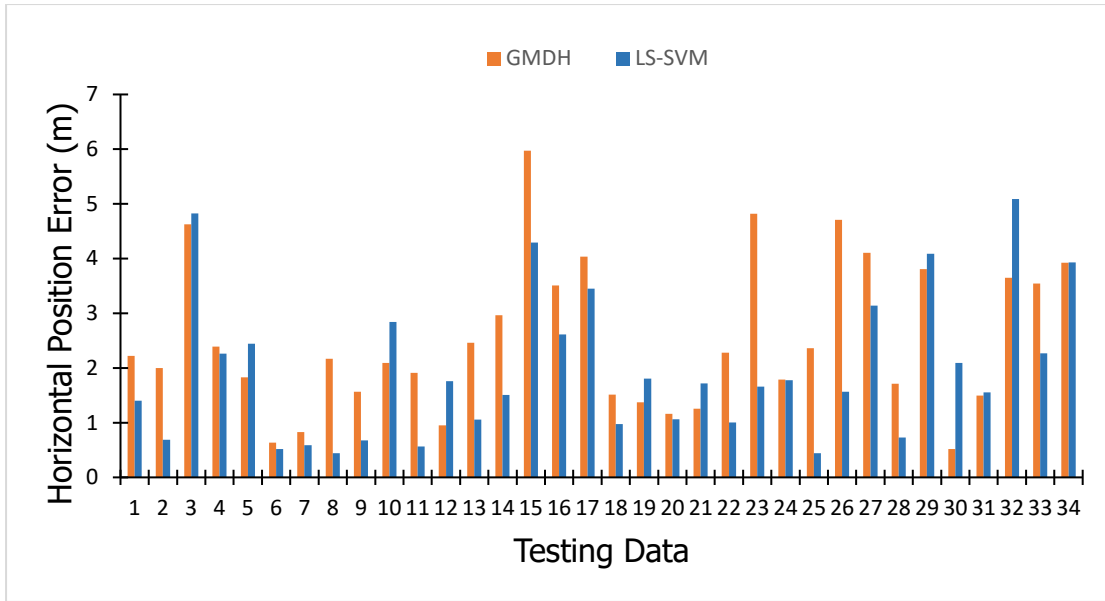


Figure 5.11 Horizontal Position Residuals for Fold 5 (Testing)

5.1.3 AI and Numerical Transformation Performance Results

In this Section, results produced by the AI models (GMDH, LS-SVM) and Bursa – Wolf are presented. The essence is to understand the dynamics of the results produced by each method and their respective strength in coordinate transformation. Therefore, the overall average performance of the AI models and the Bursa – wolf are presented in Table 5.4 and Figures 5.12 and 5.13.

Table 5.5 Performance Metric for All Folds and Models (Average)

Statistical Indicator	Average					
	Training (dd)			Testing (m)		
	BURSA-WOLF	GMDH	LS-SVM	BURSA-WOLF	GMDH	LS-SVM
RMSE HE	9.32E-06	7.24805E-06	5.9896E-06	3.339601	3.031211	2.55411
Min HE	1.06E-06	-1.46743E-06	-9.47106E-07	0.390546	-0.54464	-0.33193
Max HE	2.29E-05	1.49608E-05	1.21529E-05	8.318771	6.750357	5.407009
Mean HE	7.69E-06	6.33357E-06	5.17529E-06	2.757802	2.619101	2.190432
SD	6.57E-06	5.19646E-06	4.27519E-06	2.356277	2.139041	1.79845

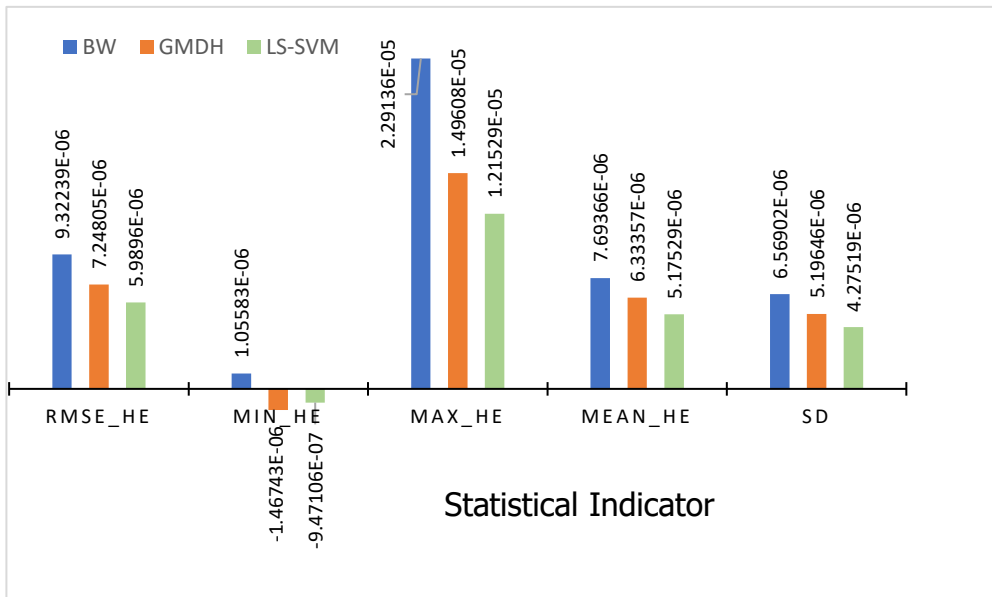


Figure 5.12 Statistical Indicators (Average) of All Folds and Model (Training)

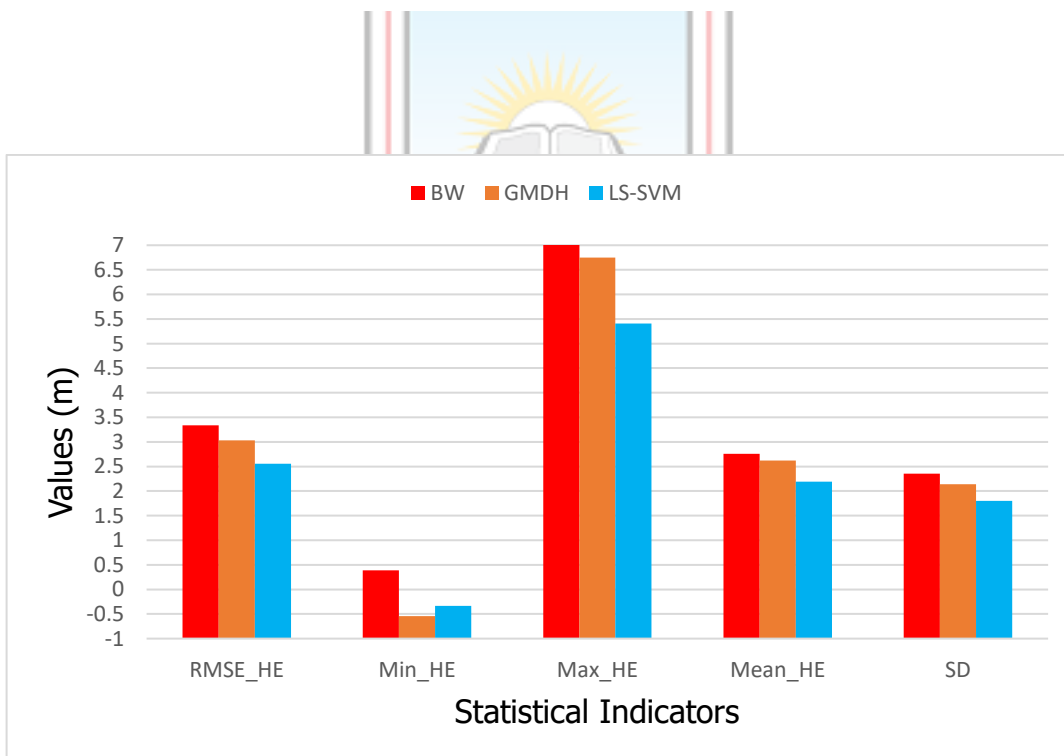


Figure 5.13 Average Plot of All Folds and Models (Testing)

5.2 Discussion

5.2.1 Bursa-Wolf Model

The seven parameters (Table 5.1) determined by the Bursa-Wolf model are three translational parameters (T_x , T_y , T_z) responsible for making the two origins coincide, three rotational parameters (R_x , R_y , R_z) responsible for making the axis of the two-datum parallel and one scale factor (sf) responsible for making the length of the axis equal in all direction. The residuals produced when estimating the parameters were the main focus of the assessment of the effectiveness of the datum transformation procedures. The (X , Y , Z) residuals are represented as V_x , V_y , and V_z (Figure 5.1). The residual shows a fairly consistent rise and fall around the threshold of zero. From visual inspection of the seven parameter conformal transformation graphs of Figure 5.1, it was seen that in the V_z component, there were a few points that were a little far from the benchmark of zero while the V_x residuals are relatively smaller than the V_y residuals which are very close to the zero. Furthermore, the standard deviation of each parameter in Table 5.1 indicates the precision of the parameter.

5.2.2 GMDH and LS-SVM Models

The instrument used to access the extent to which the GMDH and LS-SVM, transformed geodetic coordinates deviate from the actual is the horizontal positional error (HE). Tables 5.2 and 5.3 confirm the LS-SVM was better trained than the GMDH in all five folds for the model building and also performed better than the GMDH in all five folds for the model validation (Tables 5.2 and 5.3) (testing). This means, for each fold the LS-SVM was superior to the GMDH in both the training and testing process. The kernel function the LS-SVM used to give optimal performance was the RBF Kernel. The RBF predicted very well than the polynomial and linear kernels. The obtained result spelt out that the LS-SVM perform transformation more accurately than the GMDH. To further visualise the prediction superiority of LS-SVM, Figures 5.2 to 5.11 are presented. It is obvious that the LS-SVM has demonstrated greater adaptability to the different folds than the GMDH.

5.2.3 Comparison Between AI Models and Bursa-Wolf Models

In order to assess a model's overall performance for the five folds, the average of the residuals as indicated by the performance measures was found. The LS-SVM performed better (Table 5.4, Figures 5.12 and 5.13) than the GMDH and Bursa-Wolf with the $RMSE_{HE}$ of 2.5541, 3.0312 and 3.3396 respectively. These $RMSE_{HE}$ (Table 5.4) computed values display all of the uncertainties that are present throughout the integrated horizontal coordinates.

The lowest Mean HE of 2.1904 m was produced by the LS-SVM, this means that when the LS-SVM is applied to the study area, the mean horizontal position error of 2.1904 m will be obtained as compared to the GMDH of 2.6191 m and Bursa-wolf of 2.7578 m. The Mean HE (Table 5.4) value gives the achievable average horizontal positional error when a model is used, in this case, Bursa-wolf, GMDH and LS-SVM. The maximum and minimum HEs give the extent of the interval of the errors produced by the three models in this study. It is clear from Table 5.4 that the LS-SVM obtained the best minimum (-0.33193) and maximum (5.407) HE tests result. Therefore, the LS-SVM is a good choice for coordinating transformation in Ghana because of its ability to predict satisfactorily.

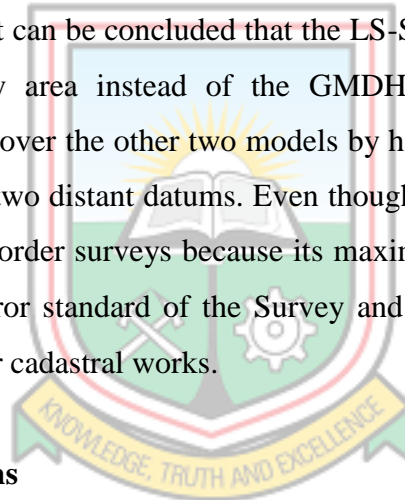
For the SD value, similar transformation precisions were determined for the five folds. The SD of each fold is not too far from each other within a fold. This means that the deviations were almost in the same range per model. The LS-SVM was the model with the lowest SD. This can be interpreted that the spread of the projected coordinates from the LS-SVM prediction is better as compared to the GMDH and the Bursa-Wolf models. Based on Table 5.4 and Figure 5.13, it can be deduced that the LS-SVM is preferable for coordinate transformation in the study area because of its best performances demonstrated in the study.

CHAPTER 6

CONCLUSIONS AND RECOMMENDATIONS

6.1 Conclusions

Coordinate transformation is still a field of interest in geoscience in Ghana because of the difference in the Accra 1929 datum and GNSS datum (WGS 84). This study applied the least square adjustment technique to derive transformation parameters based on Bursa-Wolf model. The Bursa-Wolf model was compared with the GMDH and the LS-SVM using the K-fold cross-validation for transforming coordinates. According to the results, the LS-SVM outperformed the GMDH and Bursa-Wolf models, with RMSE HE values of 2.55411, 3.031211, and 3.339601, respectively. The optimal performance of a model is gained by the K-fold cross-validation technique and not a single hold out cross validation technique. From the performance metric, it can be concluded that the LS-SVM should be used to transform coordinates in the study area instead of the GMDH or Bursa-Wolf. The LS-SVM demonstrates its strength over the other two models by handling some of the uncertainties in the data related to the two distant datums. Even though the LS-SVM performs better; it is recommended for low-order surveys because its maximum horizontal error exceeds the ± 0.9114 m allowable error standard of the Survey and Mapping Division of the Lands Commission of Ghana for cadastral works.



6.2 Recommendations

The following recommendations are made from the research:

- The survey fraternity of Ghana still uses the non-geocentric datum as its reference for surveying and mapping. Because of that, the GNSS acquired data re transformed using classical transformation results. Based on the results obtained, it is recommended that AI should be adopted for coordinate transformation specifically, the LS-SVM that produced the best results.
- To further improve the coordinate transformation results obtained in this study, it is recommended that the LS-SVM model controlling parameters must be automatically fine-tuned using bio-inspired optimization algorithms such as goat search, grey

wolf and whale optimization. This will help eliminate the manual tasking involved in the fine-tuning process during training.



REFERENCES

- AlBinHassan, N. M., and Wang, Y. (2011). Porosity Prediction Using the Group Method of Data Handling. *Geophysics*, Vol. 76, No. 5, pp. 15 - 22. <https://doi.org/10.1190/geo2010-0101.1>, Accessed: August 18, 2023.
- Amiri and Soleimani, (2021), “ML - Based Group Method of Data handling; an improvement on the conventional GMDH”, *Complex and Intelligent systems*, Vol. 7, pp. 2949 – 2960.
- Anon. (2014), “Reference Frames in Practice Manual”, Commission 5 Working Group 5.2, International Federation of Surveyor, No. 64, 68 pp.
- Annon. (2022), “Coordinate Conversions and Transformations including Formulas”, *Geomatics Guidance Note Number 7 Part 2, International Association of Oil and Gas Producers*, 2022, 174 pp.
- Assaleh, K., Shanableh, T., and Kheil, Y. A. (2013), “Group Method of Data Handling for Modelling Magnetorheological Dampers”, *Intelligent Control and Automation*, Vol 4, No. 1, pp. 70 – 79.
- Ayer, J. (2008), “Transformation Models and Procedures for Framework Integration of the Ghana national Geodetic Network”, *Ghana Surveyor*, Vol. 1, pp. 52 – 58.
- Ayer, J. and Fosu, C. (2008), “Map Coordinate Referencing and the Use of GPS Datasets in Ghana”, *Journal of Science and Technology*, Vol. 28, No. 1, pp. 116 – 127.
- Bezdek, A. and Sebera, J (2013), “MATLAB Script for 3D Visualizing Geodata on a Rotating Globe Astronomical Institute”, *Academy of Sciences of the Czech Republic, Computer and Geosciences* 56, pp. 127 – 130.
- Boon, P. S. and Setan, H. (2007), “3D Coordinate Transformation Using Molodensky Badekas Transformation Model”, *Faculty of Geosciences and Engineering, Universiti Teknologi Malaysia*, 13 pp.

- Borge, A. (2013), "Geoid Determination Over Norway Using Global Earth Gravity Models", MSc Thesis, Department of Civil and Transport Engineering, Norwegian University of Science and Technology, 72 pp.
- Clynch, J. R. (2002), "Earth Models and Maps", Naval Postgraduate School, 7 pp.
- Dakhil, A. J. (2015), "GPS Measurements and Its Impact on Geodetic Datum Maintenance", Publish MSc Thesis, Faculty of Engineering Mansoura University, 140 pp.
- Deakin, R. E. (2006a), "Bursa-wolf and Molodensky-Badekas Transformations, Lecture Notes, Department of Mathematical and Geospatial Sciences", RMIT University, 22 pp.
- Deakin, R. (2006b), "Traverse Computation on The UTM Projection for Surveys of Limited Extent", *Research Gate*, School of Mathematical and Geospatial Sciences, RMIT University, 20 pp.
- Delmelle, E. and Dezzani, R. (2015), "Classification and Selection of Map Projections for Geospatial Applications", Handbook of Research on Geoinformatics, *Research Gate*, pp. 89 - 98
- Dhungana, R. and Lama, S. (2014), "The Determination of Transformation Parameter", Project Report, Ministry of Land Reform and Management Training Centre, Government of Nepal, pp. 44.
- Dutta, S., Bandopadhyay, S., Ganguli, R and Misra, D. (2010), "Machine Learning Algorithms and their Application to Ore Reserve Estimation of Sparse and Imprecise Data", *Journal of Intelligent Learning Systems and Applications*, Vol. 2, pp. 86 -96.
- Eren, O. and Hajiyev, C. (2013), "Aircraft Position and Velocity Determination Based On GPS Measurements Using Distance Difference and Doppler Methods Aircraft Position and Velocity Determination Based On GPSA", Ankara International Aerospace Conference, Metu, Ankara Turkey, 51 pp.

Ghaderpour, E. (2015), Map Projection, Department of Earth and Space Science and Engineering, York University, 19 pp.

Ghilani, C. and D., Wolf, P. R. (2012), “*Elementary Surveying, An Introduction to Geomatics*”, 13th Edition, 983 pp.

Gomes, D. and Hut, S. (2019), Coordinate Systems And Projections (GIS), *East Timor Cartography*. 22 pp.

Hassan, A., Mustafa, E. K., Zhang, L. (2020), “Analytical Study of 3D Transformation Parameters Between WGS84 and Adindan Datum Systems in Sudan”, *Arabian Journal for Science and Engineering*, Vol 45, pp. 351 – 365.

Jessen, V. (2009), "Understanding Coordinate Reference Systems, Datums and Transformations", *International Journal of Geoinformatics*, pp. 41 - 53

Jung, Y., and Hu, J. (2015). "A K-fold averaging cross-validation procedure", *Journal of nonparametric statistics*, Vol. 27, pp 167 - 179.

Ivakhnenko, A. G. (1971), "Polynomial theory of complex systems, IEEE Transactions on Systems", *Man and Cybernetics*, Vol. 4, pp. 364 – 378.

Kumi-Boateng, B. and Ziggah, Y. Y. (2017), Horizontal Coordinate Transformation Using Artificial Neural Network Technology- A Case Study of Ghana Geodetic Reference Network, Vol 11, No. 1, 11 pp.

Kumi-Boateng and. Ziggah, Y.Y (2020a), "Empirical Study on the Integration of Total Least Squares and Radial Basis Function Neural Network for Coordinate Transformation", *Ghana Journal Of Science Technology and Development*, Vol. 7, pp. 38 - 57.

Kumi-Boateng, B. and Ziggah, Y.Y. (2020b), "Feasibility of Using Group Method of Data Handling (GMDH) Approach for Horizontal Coordinate Transformation", *Geodesy and Cartography*, Vol. 46, pp. 55 – 66.

Lantz, B. (2013), "Machine Learning with R", Packt Publishing Ltd., Birmingham B3 2PB, UK, 396 pp.

Laari, P. B., Ziggah, Y.Y., and Annan, R. F. (2016), "Determination of 3D Transformation Parameters for the Ghana Geodetic Reference Network using Ordinary Least Squares and Total Least Squares Techniques", *International Journal of Geomatics and Geosciences*, Vol. 7, No 3, pp. 225 - 261.

Mugnier, C. J. (2011), "Grids and Datums" – Republic of Ghana", pp. 201–203

Mirghasempour, M. A. and Joodaki, G. (2008), "A Modern Astro-Geodetic Approach to Determination Geoid, Case Study: Iran", *EGU General Assembly 2008*, Vol. 10, 12 pp.

Poku-Gyamfi, Y. (2009), *Establishment of GPS Reference Network in Ghana (PhD Dissertation)*, Universitat der Bundeswehr Munchen, Germany, 204 pp.

Russell, S. J and Norvig, P. (2010), *Artificial Intelligence A Modern Approach*, 3rd Edition, 1153 pp.

Shirkin, R. (2020), "*Artificial Intelligence, A Complete Beginner's Guide to Artificial Intelligence*", 2nd Edition, 102 pp.

Solomon, M. (2013), "Determination of Transformation Parameters for Montserrado County, Republic of Liberia", Published MSc Thesis, Kwame Nkrumah University of Science and Technology, 45 pp.

Subirana, J. S., Zornoza, J. M. and Hernandez-Pajares, M. (2011), *Ellipsoidal and Cartesian Coordinates Conversion*, University of Catalonia, Spain. <https://navipedia.net>, Accessed: July 25, 2023

Suykens, J. A. K., Van Gestel, T., De Brabanter, J., De Moor, B., and Vandewalle, J. (2022), "Least Squares Support Vector Machines", *World Scientific*, Singapore. <https://doi.org/10.1142/5089>. Accessed: August 4, 2023

Tierra, A., Dalazoana, R., and De Freitas, S. (2008), “Using an Artificial Neural Network to Improve the Transformation of Coordinates between Classical Geodetic Reference Frames”, *Computers and Geosciences*, Vol.34, pp. 181 – 189

Usery, E. L., Finn, M. P., and Mugnier, C. J. (2020), “Coordinate System and Projection Chapter 8, *ResearchGate*, 26 pp.

Vermeer, M. (2019), Geodesy, “*The Science Underneath*”, Department of Built Environment, School of Engineering, Aalto University, 612 pp.

Yegnanarayana, B. (2005), *Artificial neural networks*, Prentice-Hall of India Private Limited, 399 pp.

Ziggah, Y. Y., Yakubu, I., and Kumi-Boateng, B. (2016a), “Analysis of Methods for Ellipsoidal Height Estimation – The Case of a Local Geodetic Reference Network”, *Ghana Mining Journal* 16, 9 pp.

Ziggah, Y. Y., Youjian, H., Laari, P. B., and Hui Z. (2016b), Capability of Artificial Neural Network for Forward Conversion of Geodetic Coordinates (ϕ, λ, h) to Cartesian Coordinates (X, Y, Z), “*Mathematics Geosciences*”, Vol., 48, No. 6, pp. 687 - 721

Ziggah, Y. Y., Youjian, H., Hui Z., Tierra, A., Konate, A. A., (2016c), Performance Evaluation of Artificial Neural Networks for Planimetric Coordinate Transformation—A Case Study, Ghana, *Arabian Journal of Geosciences*, Vol 9, No. 17, 16 pp.

Ziggah, Y.Y. (2017), *Principles of Geodesy*, BSc Lecture Note, University of Mines and Technology, 112 pp.

Ziggah, Y. Y. and Yakubu, I. (2017), “Alternative Methods of Determining Translation Parameters for Geocentric Translation Model Applications”, *Ghana Journal of Technology*, Vol. 2, No. 1, pp. 38 - 50.

Ziggah, Y. Y., Youjian, H., Laari, P. B., and Hui, Z. (2017), “Novel Approach To Improve Geocentric Translation Model Performance Using Artificial Neural Network”, BCG – Boletim de Ciências Geodésicas, ISSN 1982-2170 pp. 213 – 233

Ziggah, Y. Y. and Laari, P. B. (2018), “Application of Multivariate Adaptive Regression Spline Approach for 2D Coordinate Transformation”, *Ghana Journal of Technology*, Vol. 2, No. 2, pp. 50 - 62.

Ziggah, Y. Y., Issaka, Y., Laari, P. B. and Hui, Z. (2018), “2D Cadastral Coordinate Transformation Using Extreme Learning Machine Technique, *Geodesy and Cartography*, Vol. 67, No. 2, pp. 321–343

Ziggah, Y. Y., Youjian, Issaka, Y., and Laari, P. B (2019a), “Least Squares Support Vector Machine Model for Coordinate Transformation”, *Geodesy and Cartography*, Vol. 45, No. 1, pp. 67-77.

Ziggah, Y. Y, Youjian, H, Tierra, A. R, Laari, P. B (2019b), “Coordinate Transformation Between Global and Local Data Based on Artificial Neural Network with K-Fold Cross-Validation in Ghana”, *Earth Science Research Journal*, Vol. 23, No. 1, pp. 67-77

Ziggah, Y. Y. (2022), *Geodesy 578*, MSc Lecture Note, University of Mines and Technology, 75 pp.

APPENDICES
APPENDIX A
COMMON POINT COORDINATES IN
WGS84 AND WAR OFFICE 1926

PT ID	WGS_LONG	WGS_LAT	WGS_HGHT	WAR_LONG	WAR_LAT	WAR_HGHT	Existing North	Existing Esating
CFP 4034	-1.278364339	5.691733211	172.245	-1.278628925	5.688938547	174.7549695	370809.85	798758.83
GCS 291	-2.858503986	5.798711592	375.572	-2.858735278	5.795919167	378.2075909	410695.84	224631.19
GCS 313	-2.606816878	7.713151233	509.369	-2.607044444	7.710441111	501.7287917	1105133.69	318400.1
CFP T9/290	-1.479260414	7.436515256	331.905	-1.479520511	7.433788356	325.2248783	1003779.62	726367.84
GCST11 58	-0.009611903	9.388786756	236.907	-0.009882914	9.386104906	219.2542619	1712402.22	1256739.81
GCS T16/3	-2.465205197	9.208804411	356.025	-2.465425878	9.206138411	340.5041899	1647693.62	371706.42
T16 24	-2.468451497	10.37967958	389.293	-2.468659928	10.37705296	367.7293126	2072618.79	372393.01
GCS T17/16	-0.447144786	10.53006745	412.344	-0.447401603	10.52742752	389.0524414	2126130.92	1098404.52
GCS T19/1	-1.520396892	9.187221242	179.987	-1.52063485	9.184545456	164.1591918	1638915.4	712314.16
GCS T20 23	-2.381942175	10.02666255	392.906	-2.382152058	10.02402293	373.1211504	1944367.85	402928.87
GCS/T21/33	-0.834197997	9.405908331	212.937	-0.834446858	9.403234806	195.6376823	1718127.86	959643.22
GCS T23 3	-2.465920092	10.67266894	339.634	-2.466129292	10.67005184	316.5678728	2178947.08	373799.37
GCS T23 14	-2.090571122	10.88084132	374.835	-2.090790286	10.87822944	350.5455134	2253931.08	508797.05
CFP 200	-0.559314619	5.625800658	304.689	-0.5595975	5.623015	307.1850974	346933.94	1060041.45
GCS 101	-0.776406814	5.315700392	151.948	-0.77668	5.312912222	156.2250924	234410.91	981195.24
GCS 114	-0.202173433	5.594222708	74.978	-0.202476164	5.591432519	77.44958277	335614.88	1189840.65
GCS 145	-1.411894256	6.556918669	503.473	-1.412160556	6.554148056	501.4241249	684673.93	750479.52
GCS CFP 205	0.49514755	6.495626231	622.703	0.494838056	6.492844167	619.954899	663176.47	1442407.83
GCS CFP 206	0.268332914	6.813044558	565.984	0.2680325	6.810275	561.6815656	778120.12	1359800.69
GCS214	0.072658269	6.131262939	51.55	0.072357778	6.128476944	50.9910714	530601.49	1289360.11
GCS 215	0.008511892	6.127742308	90.775	0.008213056	6.124956667	90.27130506	529279.26	1266069.85
CFP 217	-0.729702328	5.943109353	311.542	-0.729977778	5.940330556	312.4272474	461992.4	998070.31
GCS CFP 219	0.226219136	7.813436464	159.96	0.225936389	7.810691667	150.3957605	1141049.08	1343545.59
CFP159	-0.341338758	6.291648572	681.632	-0.341623056	6.288871389	680.4475454	588541.08	1138967.75
GCS T19/29	-1.462061325	10.80620539	298.757	-1.462294086	10.80358686	274.5632819	2226272.82	734168.62
GCS T24/1	-0.515587872	8.44390185	186.639	-0.515844644	8.441194728	174.1798858	1369227.61	1074884.01
GCS 186	-1.918489572	6.581243053	536.924	-1.918741944	6.578472222	534.9816998	693741.68	566710.73
GCS 304	-1.445335186	6.992211036	621.024	-1.445590556	6.989461667	616.6785696	842589.26	738496.56
GCS311	-1.983642275	7.685043006	562.296	-1.983886667	7.682331667	554.5375737	1094250.99	543929.66
GCS T18/24	-1.560823381	8.807884817	187.463	-1.561067222	8.805198656	173.6274151	1501316.72	697527.39
GCS T20/12	-1.309380403	9.519088828	163.346	-1.309619322	9.516423161	145.6972063	1759225.61	788490.69
GCS 188	-2.352255867	6.431666969	591.945	-2.352508333	6.428902778	590.9893184	639831.96	409185.48
GCS 189	-2.093713133	6.306801236	573.85	-2.093962778	6.304021944	573.4483858	594302.37	502926.12
GCS 207	-1.966148986	5.849619928	400.65	-1.966403611	5.846824167	402.6362252	428353.9	548934.64

APPENDIX B

BURSA-WOLF CODE

```

clc
clear
close all
format long % results to be in 15 decimal places 0

% Bursa-Wolf Model
DATA = readmatrix('Full_DataBW1');

% reading the WGS84 Ellipsoidal Data
WGS_Long = DATA(:,1);
WGS_Lat = DATA(:,2);
WGS_h = DATA(:,3);

% reading the War office 1926 Ellipsoid Data
W_Long = DATA(:,4);
W_Lat = DATA(:,5);
W_h = DATA(:,6);

%%Defining the ellipsoidal parameters of the War Office Ellipsoid
awar = 6378299.99899832;
fwar = 1/296; %
ewar = sqrt((2*fwar)-fwar^2);
bwar = 6356751.68824042;

% conversion of War office geodetic coordinates to cartesian X, Y, Z coordinates
for i = 1:34
    nw(i,1)=(ewar*sind(W_Lat(i)))^2;
    RP(i,1)= awar/(sqrt(1 - nw(i,1)));
end

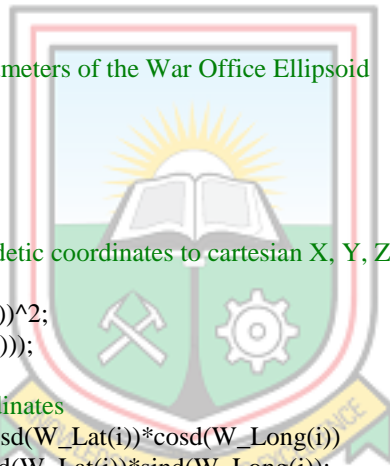
% computing the cartesian coordinates
XWAR(i,1) = (RP(i) + _h(i))*cosd(W_Lat(i))*cosd(W_Long(i))
YWAR(i,1) = (RP(i) + h(i))*cosd(W_Lat(i))*sind(W_Long(i));
ZWAR(i,1) = ((RP(i)*(1-(ewar)^2))+ W_h(i))*sind(W_Lat(i));
end

%%Defining the ellipsoidal parameters of the WGS84 Ellipsoid
aWGS = 6378137.000;
fWGS = 1/298.257223563;
eWGS = sqrt((2*fWGS)-fWGS^2);
bWGS = 6356752.314245;

% conversion of WGS84 coordinates to cartesian X, Y, Z coordinates
for a = 1:34
    ng(a,1) = (eWGS*sind(WGS_Lat(a)))^2;
    gRP(a,1) = aWGS/(sqrt(1 - ng(a,1)));
end

% computing the cartesian coordinates
XWGS(a,1)=(gRP(a)+WGS_h(a))*cosd(WGS_Lat(a))*cosd(WGS_Long(a));
YWGS(a,1)=(gRP(a)+WGS_h(a))*cosd(WGS_Lat(a))*sind(WGS_Long(a));
ZWGS(a,1)=(gRP(a)*(1-(eWGS)^2))+WGS_h(a))*sind(WGS_Lat(a));
end

```



```
% formulating the design matrix (A)
```

```
A = zeros(34*3,7);
```

```
for i = 1:34
```

```
    A(i*3-2,1)=1;
```

```
    A(i*3-2,5)= -ZWAR(i);
```

```
    A(i*3-2,6)= YWAR(i);
```

```
    A(i*3-2,7)= XWAR(i);
```

```
    A(i*3-1,2)= 1;
```

```
    A(i*3-1,4)= ZWAR(i);
```

```
    A(i*3-1,6)= -XWAR(i);
```

```
    A(i*3-1,7)= YWAR(i);
```

```
    A(i*3,3)= 1;
```

```
    A(i*3,4)= -YWAR(i);
```

```
    A(i*3,5)= XWAR(i);
```

```
    A(i*3,7)= ZWAR(i);
```

```
End
```

```
L=zeros(34*3,1);
```

```
for i = 1:34
```

```
    L(i*3-2,1) = XWGS(i)-XWAR(i);
```

```
    L(i*3-1,1) = YWGS(i)-YWAR(i);
```

```
    L(i*3,1) = ZWGS(i)-ZWAR(i);
```

```
End
```

```
Qxx = inv(A'*A);
```

```
x = Qxx*A'*L;
```

```
%t = A'*L;
```

```
%XX = (A'*A)\t;
```

```
%X = (A'*A)\(A'*L);
```

```
% defining the translation parameters
```

```
Dx = x(1);
```

```
Dy = x(2);
```

```
Dz = x(3);
```

```
% defining the rotation parameters
```

```
Rx = ((180/pi)*3600)*x(4);
```

```
Ry = ((180/pi)*3600)*x(5);
```

```
Rz = ((180/pi)*3600)*x(6);
```

```
% defining the scale factor
```

```
Sf = 1000000*x(7);
```

```
% calculate residuals
```

```
V = (A*x)-L;
```

```
% calculate for standard deviation
```

```
n = 34; % number of observations
```

```
u = 7; % number of unknown parameters
```

```
SD = sqrt((V'*V)/(3*n-u));
```

```
% calculate for variance
```

```
VAR = (SD)^2;
```

```
%calculate the standard deviation for each transformation parameter
```

```
S = SD*sqrt(diag(Qxx));
```



```

% definig parameters
parameters = [Dx;Dy;Dz;x(4);x(5);x(6);x(7)];
yI = A*parameters;

% perform the transformation
for i = 1:34
    Xw(i,1)=XWGS(i)-yI(i*3-2,1);
    Yw(i,1)=YWGS(i)-yI(i*3-1,1);
    Zw(i,1)=ZWGS(i)-yI(i*3,1);
End

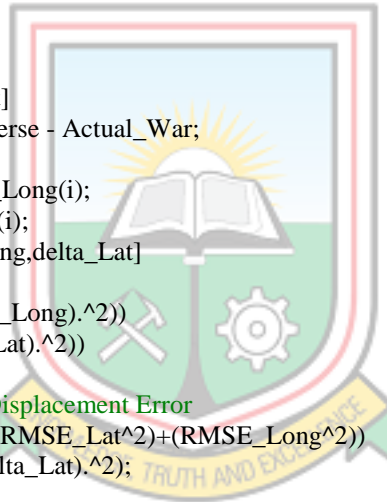
% Reverse Conversion
for n = 1:34
    n_Long(n,1) = atand(Yw(n) / Xw(n));
end

for i = 1:34
    pd(i,1) = sqrt(((Xw(i))^2)+((Yw(i))^2));
    sec_ecc = ((ewar)^2)/(1 - (ewar)^2);
    w(i,1) = atand((awar*Zw(i))/(bwar*pd(i)));
    n_Lat(i,1) = atand((Zw(i) + (bwar*sec_ecc)*(sind(w(i))^3))/(pd(i)-(awar*((ewar)^2))*cosd(w(i))^3));
    n_h(i,1) = (pd(i)/cosd(n_Lat(i))) - RP(i);
end

Reverse = [n_Long,n_Lat]
Actual_War = [W_Long,W_Lat]
Residual_Transformtion = Reverse - Actual_War;
for i=1:34
delta_Long(i,1) = W_Long(i)-n_Long(i);
delta_Lat(i,1) = W_Lat(i)-n_Lat(i);
Projection_Residual = [delta_Long,delta_Lat]
end
RMSE_Long = sqrt(mean((delta_Long).^2))
RMSE_Lat = sqrt(mean((delta_Lat).^2))

%%Computing the Horizontal Displacement Error
RMSE_Horizontal_Error =sqrt((RMSE_Lat^2)+(RMSE_Long^2))
HE = sqrt((delta_Long).^2 +(delta_Lat).^2);
Mim_HE = min(HE);
Max_HE = max(HE);
mean_HE = mean(HE);
SD = std(HE);

```



APPENDIX C

GROUP METHOD DATA HANDLING CODE

```
clc
clear all
format short

%%READING THE EXCEL DATA
Training_Data = readmatrix('Training_Data1');
Testing_Data = readmatrix('Full_Data');

%%TRAINING DATA
Xtr = Training_Data(:,1:3);
Ytr = Training_Data(:,4);

%%TESTING DATA
Xts = Testing_Data(:,1:3);
Yts = Testing_Data(:,4);

%%FORMING THE GMDH TRAINING MODEL
[model, time] = gmdhbuild(Xtr, Ytr);

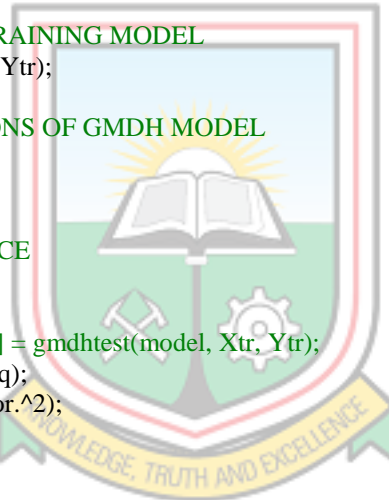
%%OUTPUTS THE EQUATIONS OF GMDH MODEL
precision = 12;
gmdheq(model, precision)

%%TRAINING PERFORMANCE
Yq = gmdhpredict(model, Xtr);

%%[MSE, RMSE, RRMSE, R2] = gmdhstest(model, Xtr, Ytr);
training_error = gsubtract(Ytr, Yq);
train_MSE = mean(training_error.^2);
train_RMSE = sqrt(train_MSE);
train_SD = std(training_error)

%%TESTING PERFORMANCE
Ytest = gmdhpredict(model, Xts); %% TESTING TARGET PREDICTIONS

%%[MSE_test, RMSE_test, RRMSE_test, R2_test] = gmdhstest(model, Xts, Yts);
test_error = gsubtract(Yts, Ytest);
test_MSE = mean(test_error.^2);
test_RMSE = sqrt(test_MSE);
test_SD = std(test_error)
```



APPENDIX D

LEAST SQUARE SUPPORT VECTOR MACHINE CODE

```
clc
format long

%%READING THE EXCEL DATA
Training_Data = readmatrix('Training_Data5')
Testing_Data = readmatrix('Full_Data');

%%TRAINING DATA
X = Training_Data(:,1:3)
Y = Training_Data(:,5);

%%TESTING DATA
Xt = Testing_Data(:,1:3);
Yobs = Testing_Data(:,5);

%%FORMING THE LS-SVM TRAINED MODEL
type = 'f';%%f means function estimation
kernel = 'RBF_kernel';%%lin_kernel, poly_kernel, RBF_kernel

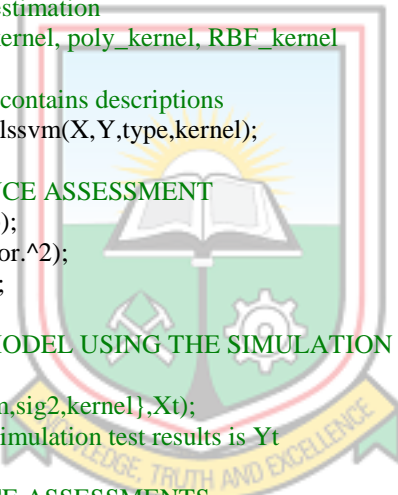
%%Yp is the output and model contains descriptions
[Yp,alpha,b,gam,sig2,model] = lssvm(X,Y,type,kernel);

%%TRAINING PERFORMANCE ASSESSMENT
training_error = gsubtract(Y,Yp);
train_MSE = mean(training_error.^2);
train_RMSE = sqrt(train_MSE);

%%TESTING THE LS-SVR MODEL USING THE SIMULATION FUNCTION

% Yt = simlssvm({X,Y,type,gam,sig2,kernel},Xt);
Yt = simlssvm(model,Xt);%%Simulation test results is Yt

%%TESTING PERFORMANCE ASSESSMENTS
test_error = gsubtract(Yobs,Yt);
test_MSE = mean(test_error.^2);
test_RMSE = sqrt(test_MSE)
```



APPENDIX E

PROJECTION CODE

```

clc
format long
clear
close all

%Reading data
DATA = readmatrix('Projection5');

Long = DATA(:,1);
Lat = DATA(:,2);
Actual_North = DATA(:,3);
Actual_East = DATA(:,4);

% conversion of new war office coordinates in degrees into radians
N_Long = deg2rad(Long);
N_Lat = deg2rad(Lat);
%N_H = deg2rad(N_h);

% transforming coordinates to projected grid coordinates based on
% tranverse marcator of Ghana
lat2 = dms2degrees([4 40 0]);
long2 = dms2degrees([-1 00 0]);
lat0 = deg2rad(lat2);
long0 = deg2rad(long2);
N0 = 0; %%False Northings
E0 = 274319.7362; %False Eastings in metres

M0 = 516011.5389; %%
K0 = 0.99975; %scale factor at central meridian
ma = 6378299.996; %major axis
esq = 0.006745343; %eccentricity squared
feet = 0.304799706846; %%feet conversion factor
lat2 = dms2degrees([4 40 0]); %%Latitude of origin
long2 = dms2degrees([-1 00 0]);%%Meridian of origin
lat0 = deg2rad(lat2);%%convert Latitude of origin to degree
long0 = deg2rad(long2);%%convert median of origin to degree
N0 = 0; %%False Northings
E0 = 274319.7362; %False Eastings in metres
M0 = 516011.5389; %%
K0 = 0.99975; %scale factor at central meridian
ma = 6378299.996; %major axis
esq = 0.006745343; %eccentricity squared
feet = 0.304799706846; %%feet conversion factor

for i = 1:34
p(i,1) = (ma*(1-esq))/(((1-esq*(sin(N_Lat(i,1)))^2)))^(3/2);

v(i,1) = ma/sqrt(1-esq*(sin((N_Lat(i,1))))^2);

n(i,1) = v(i,1)/p(i,1);

T(i,1) = tan(N_Lat(i,1));

```



```

w(i,1) = N_Long(i,1)-long0;

A0(i,1)= (1-(esq/4)-((3*esq^2)/64)-((5*esq^3)/256));

A2(i,1)= (3/8)*(esq+((esq^2)/4)+((15*esq^3)/128));

A4(i,1) = (15/256)*(esq^2+((3*(esq^3))/4));

A6(i,1) = ((35*(esq^6))/3072);

m(i,1) = ma*((A0(i,1)*N_Lat(i,1))-(A2(i,1)*sin(2*N_Lat(i,1)))+(A4(i,1)*sin(4*N_Lat(i,1)))-
(A6(i,1)*sin(6*N_Lat(i,1))));

I(i,1) = ((w(i,1)^2)/2)*(v(i,1)*sin(N_Lat(i,1))*cos(N_Lat(i,1)));

II(i,1) = ((w(i,1)^4)/24)*(v(i,1)*sin(N_Lat(i,1))*((cos(N_Lat(i,1)))^3)*(4*(n(i,1)^2)+w(i,1)-T(i,1)^2));

III(i,1) = ((w(i,1)^6)/720)*(v(i,1)*sin(N_Lat(i,1))*((cos(N_Lat(i,1)))^5)*(8*(n(i,1)^4)*(11-(24*T(i,1)^2)) -
(28*n(i,1)^3)*(1 - (6*T(i,1)^2)) + ((n(i,1)^2)*(1-(32*T(i,1)^2))) - (n(i,1)*(2*T(i,1)^2)) + (T(i,1)^2)));

IV(i,1) = ((w(i,1)^8)/40320)*(v(i,1)*sin(N_Lat(i,1))*((cos(N_Lat(i,1)))^7)*(1385 -
(3111*T(i,1)^2)+(543*T(i,1)^4)-(T(i,1)^6)));

V(i,1) = ((w(i,1)^2)/6)*(((cos(N_Lat(i,1)))^2)*(n(i,1)-T(i,1)^2));

VI(i,1) = ((w(i,1)^4)/120)*(((cos(N_Lat(i,1)))^4)*((4*n(i,1)^3)*(1-6*(T(i,1)^2))+((n(i,1)^2)*(1 +
8*(T(i,1)^2)))-(n(i,1)*2*(T(i,1)^2)+(T(i,1)^4)));

VII(i,1) = ((w(i,1)^6)/5040)*(((cos(N_Lat(i,1)))^6)*(61-(479*T(i,1)^2)+(179*T(i,1)^4)-(T(i,1)^6)));

Nm(i,1) = (N0 + K0 * (m(i,1) - M0 + I(i,1) + II(i,1) + III(i,1) + IV(i,1))); %% Northing coordinates in metres

Em(i,1) = E0+K0*v(i,1)*w(i,1)*cos(N_Lat(i,1))*(1+V(i,1)+VI(i,1)+VII(i,1)); %% Easting -metres

Nf(i,1) = Nm(i,1)/feet; %% Northing coordinates in feet

Ef(i,1) = Em(i,1)/feet; %% Easting coordinates in feet
end

%% Computing the Error difference between the transformed and existing Easting and
%% Northing
for i=1:34
delta_North(i,1) = Actual_North(i)-Nf(i); %% Error in feet
delta_East(i,1) = Actual_East(i)-Ef(i); %% Error in feet
Projection_Residual = [delta_North,delta_East]
end

%% Computing the Root Mean Squared Error of the Easting and Northing
RMSE_N = sqrt(mean((delta_North).^2))
RMSE_E = sqrt(mean((delta_East).^2))

%% Computing the Horizontal Displacement Error
HE = sqrt((delta_North).^2 +(delta_East).^2)
Mim_HE = min(HE)
Max_HE = max(HE)
mean_HE = mean(HE)
RMSE_Horizontal_Error =sqrt((RMSE_E^2)+(RMSE_N^2))

```

Index

A

ability, 2, 19–20, 27–28, 49
accuracy, 16, 24, 26–27
application, 2, 28–29, 53, 57
approaches, modern, 27
approximations, 8, 22
Artificial Intelligence, 2, 18, 55
Artificial Neural Network, 18, 28, 56–57
artificial neurons, 18
Ayer, 1, 52
azimuthal projections, 21

B

Back Propagation Neuron Network. *See*
BPNN
Bayesian information criterion (BIC), 28
bias, 19, 28, 36–37
BPNN (Back Propagation Neuron Network),
26–29
Bursa, 17, 33, 46

C

cartesian coordinates, 15, 21, 26, 32, 35, 56,
59
Cartesian coordinate system, 13–14
Cartographers, 21
cell body, 18–19
centre meridian, 23
Clarke, 5, 8
classical methods, 26–27
classical models, 29, 32, 35
classical transformation results, 50
climate, 3, 5
Clynch, 7, 53
conformal models, 27
common points, 3, 30
complicated curves, 23
computer science, 18
concave, 23
conformal models, 27
conformal transformation models, 16
conical, 21
Conventional Terrestrial Pole (CTP), 14
conversion, 15, 59, 64

Coordinate Conversions, 15, 52
coordinates, 1, 6, 12, 15–17, 24, 26, 28, 30,
35, 37–38, 56, 59
anticipated, 38
converting, 26
false Northing, 24
map projection's, 22
negative, 5, 24
predicted, 35, 37
recorded, 35
rectangular, 33
targeted grid, 38
transfer, 16
transform, 2, 50
transformed, 32, 37
transformed estimated, 34
transformed geodetic, 48
Coordinates Operation and Map Projection,
3
coordinate system, 10, 12–13, 15, 17, 54
accessible three-dimensional, 14
global, 14
three-dimensional, 13
universal, 14
Coordinate System in Geodesy, 12
coordinate transformation, 1–2, 15–16, 20,
26–28, 32, 46, 49–50, 52, 54, 56–57
categorized, 16
conformal, 17
executing, 29
performed, 28
cross-validation approach, k-fold, 40
CTP (Conventional Terrestrial Pole), 14

D

Dakhil, 11–12, 53
datum transformation, 16
datum transformation procedures, 48
Deakin, 17, 24, 53
Delmelle, 21–22, 53
dendrites, 18
design matrix, 33–34, 60
Dezzani, 21–22, 53
distances, 21–22

distortion, 1–2, 16, 21–22, 24, 27

E

earth, 7–9, 11, 21, 23, 54
earth-centred earth-fixed (ECEF), 14
Easting, 12, 30, 37, 65
eccentricity, 8, 33, 35, 64
ECM (Error Compensation Model), 27
effectiveness of coordinate transformation, 28
eighty degrees, hundred, 24
elevations, 11
ellipsoid, 1, 5, 8–9, 22
ELM (Extreme learning machine), 27
Engineering, 52, 54, 56
Equation, 9, 17, 21, 24, 32–37
equator, 13–14, 22–24
Eren, 13–14, 53
error, 2, 7, 27, 38, 49–50, 61–63, 65
 horizontal, 37, 50
estimation performance in coordinate transformation, 28
Extreme learning machine (ELM), 27

F

False Eastings, 5, 24, 64
first step in coordinate transformation, 15
first step of coordinate transformation, 32
five folds, 35–36, 40, 48–49
Five Folds Cross Validation Technique
 Structure Numbers First, 36
Folds and Models, 46–47
Forward Conversion, 15, 32, 56
framework, 10
 coordinate, 10
functional model, 20

G

Generalized Regression Neural Network (GRNN), 27
geocentric coordinate system, 13–14
geocentric model, 16
geocentric translation model, 1, 26
geodetic, 9, 11, 13–15
geodetic coordinates, 3, 15, 21, 24, 34, 56
geodetic datums for cadastral activities, 5

geodetic reference frame, 28
geographic coordinates, predicted, 32
Geography Coordinates, 24
geoid, 7–9, 11
geoid model, 9
geometry, 17
geometry of Bursa-Wolf model, 17
Geosciences, 1, 10, 18–19, 50, 52, 55–56
geoscientists, 12–13
Ghana geodetic reference frame, 27
Ghana's cadastral survey's accuracy requirements, 28
Global Navigation Satellite System (GNSS), 1, 16, 50
Global Positioning System (GPS), 9, 16
globe, 7, 21–23
GMDH (Group Method of Data Handling), 2, 19, 28, 31–32, 35, 40–50, 52, 54
GNSS (Global Navigation Satellite System), 1, 16, 50
GNSS Coordinate System, 13–14
Gomes, 22–23, 54
GPS (Global Positioning System), 9, 16
graphs, parameter conformal transformation, 48
GRNN (Generalized Regression Neural Network), 27
Group Method, 2, 19, 35, 52, 54
Group Method of Data Handling. *See* GMDH

H

Hajiyev, 13–14, 53
HCV (Hold-out Cross Validation), 28, 36
height, 5, 9–13
 ellipsoidal, 9, 14
 orthometric, 9
Hold-out Cross Validation (HCV), 28, 36
horizontal coordinates, 10
 integrated, 49
Horizontal datums, 10
horizontal positional assessments, k-fold, 40
horizontal positional error, 38, 48–49
Horizontal Position Error, 26, 28, 37, 41–46, 49

Horizontal Position Residuals for Fold,
41–46
Horizontal Residual's Performance Metric,
40–41
Hut, 22–23, 54

I

Indicator, 41, 46
intersection, 13–14
Issaka, 57
Ivakhnenko, 19, 54

J

Jessen, 8, 11, 54

K

K-fold Cross Validation (KCV), 28, 36
Kumi-Boateng and Ziggah, 1–2, 5–6, 19–20,
27–28, 34–35
Kwahu plateau, 4

L

Laari, 1, 16, 33, 55–57
Lat, 21, 59, 61, 64–65
learning, machine, 18

M

machine learning models, 29
Map of Ghana Showing, 31
maps, 4, 7, 12, 21–24, 53
regional, 4
mathematical, 21, 53
mathematical models, 1, 24
matrix, 33–34
Mercator, 22
Mercator Projection, 22–23
meridians, 13, 22–23
central, 5, 23–24, 64
meters, 24, 40
model development, 40
model parameters, 20
Model Performance, 36

N

network, 10, 16, 18, 35
local geodetic reference, 28, 56

vertical control, 10
northings, 12, 30, 37, 65
numerical models for coordinate
transformation, 2
Numerical transformation model, 2
Numerical Transformation Model Results,
39
Numerical Transformation Performance
Results, 46

O

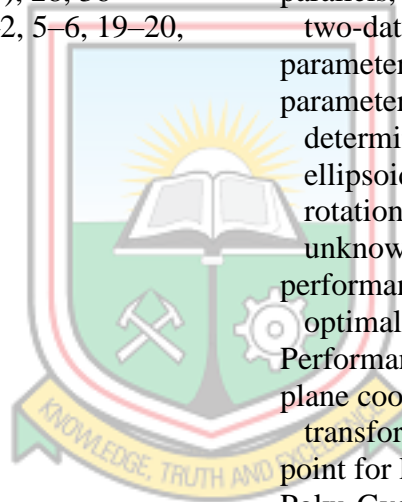
objects, 13
origin, 1, 6, 14, 17, 48, 64
true, 24

P

parallels, 12–13, 22–23
two-datum, 48
parameter conformal model, 32
parameters, 2, 8, 17, 26–27, 39, 48, 50, 61
determined, 3, 33, 39
ellipsoidal, 59
rotation, 17, 60
unknown, 33–34, 60
performance, 26–28, 49
optimal model, 37
Performance Metric for Fold, 40
plane coordinates, 21, 26
transform, 26–27
point for latitude and longitude, 5
Poku-Gyamfi, 1, 5, 55
poles, 7–8, 22–23
power, thinking, 18
precision, 36, 38, 48, 62
principles of coordinate systems, 12
priority in-terms, 26
priority in-terms of model selection for
coordinate transformation, 26
projected coordinates, 15, 24, 30, 49
calculated, 34
projection, 5, 22–23, 54, 61, 64–65
projection surfaces, 21–22

R

Radial Basis function. *See* RBF
Radial Basis Function Neural Network for



RBF (Radial Basis function), 26, 28, 36, 48,
 54, 63
 Real Earth, 7–8
 recommendations, 3, 50
 reference ellipsoid, 11–12, 15
 Reference Frames, 1, 16, 52
 reference surface, 9–11
 regional map of Ghana in Figure, 4
 regions, 5, 30
 relationship, 18–19, 21, 33
 residuals, 37, 39, 48–49, 60
 resources, 3, 30
 respective strength in coordinate
 transformation, 46
 Reverse Conversion, 15, 61
 revolution, 8
 rivers, 4–5

S

scale, 17, 22–23
 scale factor, 6, 22, 34, 48, 60, 64
 –50
 surface, 8, 21
 surveyors, 11–12, 52
 synapses, 18–19
 systems, 5, 11, 13–17, 20, 37, 54
 local, 16

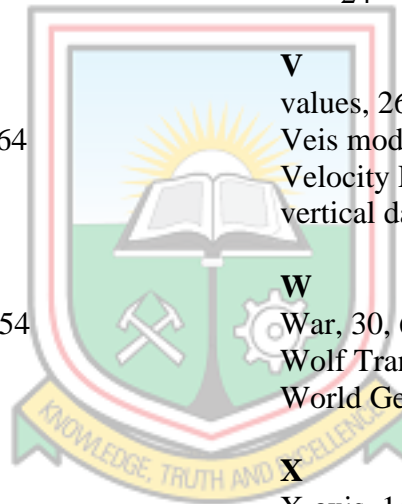
T

technique, 19–20, 26, 28, 36
 hybrid, 28
 squares, 33–34
 Technology, 1, 18, 52–53, 55–57
 Testing, 36, 40–41, 44–47, 62–63
 TLS (total least square), 28, 54–55
 TM. *See* Transverse Mercator
 tool, 26–27
 topography, 3–4
 total least square. *See* TLS
 train, 2, 62–63
 transformation models, 1, 17, 52
 best, 2, 32
 seven-parameter, 33
 traditional, 2
 transformation parameters, 1–2, 31, 33–34,
 39, 50, 53–55, 60

estimated, 34
 transformation result, reliable, 27
 transforming plane coordinates, 26
 Transverse Mercator (TM), 5, 15, 24, 32,
 35–36
 Transverse Mercator Projection, 23
 Trial, 36

U

unit, 39–40
 Universal Transverse Mercator. *See* UTM
 Universal Transverse Mercator Projection,
 24
 University, 55–57
 Usury, 21–23, 56
 UTM (Universal Transverse Mercator), 15,
 24



V

values, 26, 37, 39, 47, 49–50
 Veis model, 16
 Velocity Determination Based, 53
 vertical datum, 10–11

W

War, 30, 61
 Wolf Transformation, 17, 33
 World Geodetic System, 1, 14

X

X-axis, 14

Y

Yakubu, 1, 32, 56

Z

Ziggah and Laari, 16
 zone, 24